UNIVERSITÀ DEGLI STUDI DI TORINO

International Geology Review, 2015
Vol. 57, No. 15, 1889–1921, http://dx.doi.org/10.1080/00206814.2015.1033655

Geometry and impact of transpressional faulting in polyphasic metamorphic orogenic belts: the Viù Deformation Zone (inner Western Alps)

Perrone Gianluigi(*)

Department of Earth Sciences - University of Turin, Via Valperga Caluso, 35 – 10024 Torino (Italy); tel. +390116705187; gianluigi.perrone@unito.it

Cadoppi Paola

Department of Earth Sciences - University of Turin, Via Valperga Caluso, 35 – 10024 Torino (Italy); paola.cadoppi@unito.it

Research Centre on Natural Risks in Mountain and Hilly Enviroments (NatRisk) - University of Turin

Tallone Sergio

CNR- Institute of Geosciences and Earth Resources – Turin Unit, Via Valperga Caluso, 35 – 10024 Torino (Italy); s.tallone@csg.to.cnr.it

Corresponding author: PERRONE Gianluigi

Acknowledgmens: This work was supported by the University of Turin under Grant ex-60% (responsible: Festa A.) and by the CNR Italy –Institute of Geosciences and Earth Resources under Grant Geodinamica ed Evoluzione della Litosfera Continentale (responsible: Piana F.)

Abstract

This paper describes the geometry, structural architecture of the Viù Deformation Zone (VDZ), a brittle-ductile to brittle structure affecting the metamorphic units of the inner Western Alps, and its role in modifying the pre-existing syn-metamorphic structural setting. The VDZ reactivates and displaces the contact between two different oceanic units, the Lanzo Ultramafic Complex and the Lower Susa-Lanzo valleys Unit, characterized by a polyphasic syn-metamorphic deformation. It shows a strike-slip duplexes geometry, constituted by N-S reverse-dextral faults linked by NW-SE antithetical sinistral-reverse faults, and represents a contractional step-over zone along an N-S regional dextral-reverse structure, the Col del Lis-Trana Deformation Zone.

The activity of these transpressional structures caused the steepening of the Lanzo Ultramafic Complex and drove the last stages of its exhumation. The 3D geometry of the VDZ seems to have been strongly controlled by the reactivation of different pre-existing anisotropies, like the buried western edge of the Ivrea body and the metamorphic foliations. Brittle reactivation also induced blocks rotation mechanism along this structure, causing anomalous kinematic relations between the VDZ associated faults.

This study, hence, shows that in metamorphic orogens the mechanisms generating strike-slip duplexes may be different from those classically provided by literature, with brittle reactivation and blocks rotation strongly prevailing on newly formed faults. In such orogens, moreover, rotations induced by transpressional faulting may be sometimes mistaken with steep syn-metamorphic shear zones. Therefore, the overlook and the underestimation of the effects of the brittle deformations and of its associated rotations may cause erroneous interpretation in the tectonic reconstructions

Keywords: faulting, transpression, strike-slip duplex, blocks rotation, brittle reactivation, Western Alps

1. Introduction

Transpressional faulting (Harland 1971) is observed at all scales, from plate-margin (Lu and Malavieille 1994; Teyssier *et al.*, 1995; Goldfinger *et al.* 1997) to metre and centimetre-scale (Goodwin and Williams 1996; Tikoff and Greene 1997; Lin *et al.* 1998; Holdsworth *et al.* 2002a; Tavarnelli 1998; Tavarnelli and Holdsworth 1999; Tavarnelli *et al.* 2004), where oblique convergence between different blocks or step-over and bending along transcurrent faults (Woodcock and Fischer 1986) occurs.

The 3D geometry of transpressional faulting has been investigated through field-, experimental-, seismic-based and theoretical studies (Wilcox *et al.* 1973; Sanderson and Marchini 1984; Harding 1985; Naylor *et al.* 1986; Sylvester 1988; Tavarnelli and Pasqui 2000; Bonora and McClay 2001; Woodcock and Rickards 2003). These studies showed that the transpressional deformation is characterized by some distinctive features such as the map-view imbricate fault patterns that define open fans or closed duplexes (Fig. 1; Woodcock and Fischer 1986) varying in shape from lozenge to rhomboidal (Bonora and McClay 2001).

In cross-sections, transpressional faults mainly show flower structure geometry (Wilcox *et al.* 1973), which comprise upward-diverging faults, typically cutting antiformal push-up structures (Fig. 1). Sometimes strongly asymmetric flower structures, characterized by steep transpressional faults displacing a monocline with a sub-vertical limb are also observed (Fig. 1b; Woodcock and Rickards 2003).

Transpressional deformation is also commonly associated with the partitioning of the bulk strain into distinct domains characterized by orogen parallel strike-slip and reverse faults (Oldow *et al.* 1990; Molnar 1992; Tikoff and Teyssier 1994; Jones and Tanner 1995; Teyssier *et al.* 1995; Dewey *et al.* 1998; Jiang *et al.* 2001; Holdsworth *et al.* 2002b; Jones *et al.* 2004).

Kinematic partitioning can be controlled by a number of parameters, such as the lithosphere-scale boundary conditions (e.g. Oldow *et al.* 1990; Molnar 1992; Teyssier *et al.* 1995; Tavarnelli 1998; Tikoff *et al.* 2002), rheology of the orogenic wedge (Platt 1993), occurrence of pre-existing weak anisotropies, such as faults (Mount and Suppe 1987; Zoback and Healy 1992; Jones and Tanner 1995; Vauchez *et al.* 1998; Woodcock and Rickards 2003), or the proximity to an oblique converging indentor (Jezek *et al.* 2002; Sue and Tricart 2003; Perrone *et al.* 2010, 2011a; Fusetti *et al.* 2012).

In metamorphic orogenic belts, the paucity of reliable geological markers and the severe syn-metamorphic tectonic deformation could prevent the acquisition of useful information for a complete understanding of the role played by post-metamorphic tectonic stages in the final assembly of such orogens. However, the distinctive geometry of post-metamorphic transpressional faults may be useful for an enhanced understanding of their kinematics and role played in deforming the previous syn-metamorphic setting (see, e.g., Storti *et al.* 2006, Perello *et al.* 1999; 2001; Claypool *et al.* 2002; Sue and Tricart 2003; Perrone *et al.* 2011a).

It is worthed to remind that brittle transpressional tectonics may cause blocks rotation, both in the vertical and horizontal plane, sensibly modifying the syn-metamorphic structural setting. If block rotation is neglected, erroneous interpretations in the tectonic reconstructions may usually occur, especially regarding the earliest orogenic phases.

This may be the case of the most internal sector of the Western Alps (Italy) where only in the last few years structural studies focussed on its post-metamorphic tectonic evolution (Agard *et al.* 2003; Balestro *et al.* 2009; Malusà *et al.* 2009; Perrone *et al.* 2010, 2011a, b, 2013). Wide sectors of this part of the chain still lack a detailed analysis of the geological structures related to this phase, of their impact on the pre-existing tectonic setting and, consequently, of the mechanisms that drove the last stages of the exhumation of metamorphic units.

In this paper, detailed field mapping (1:10,000 scale), morpho-structural analysis and structural analysis of both syn- and post-metamorphic structures carried out in the inner Grain Alps (italian Western Alps, Fig. 2) allowed to show in detail the geometry, kinematics and the role played by a regional late- to post-metamorphic transpressional structure, the Viù Deformation Zone (VDZ hereafter) in deforming and reorganizing the pre-existing structural setting. This latter was entirely attributed in the literature (Nicolas 1966; Nicolas *et al.* 1972) to deformation related with a major ductile left-lateral shear zone (the Viù Locana-Zone), which represented one of the major ductile shear zones that drove the early stages of the Alpine tectonic history (Ricou and Siddans 1986; Coward and Dietrich 1989). Therefore, the results of this study will be discussed in the frame of the post-Oligocene tectonic evolution of the Western Alps and compared with the previous interpretations. Moreover, the influence of the inherited structures on the development and the 3D geometry of the VDZ will be discussed and compared with the classical models proposed for the transcurrent/transpressive faults.

In the following we will use the term ‘fault’ to refer to a single fault segment, and ‘fault population’ to refer to arrays of roughly contemporaneous faults. Moreover, under the general term of “deformation zone”, we refer to a regional, highly strained domain damage zone, several kilometres in length and about one kilometre wide, which was subject to polyphasic kinematic evolution.

Figure 1 here

2. Geological setting

2.1. Regional framework

In the NW Italy two orogenic belts are present: the Western Alps and the Northern Apennines. The deposits of the Tertiary Piedmont Basin (TPB in Fig. 2) and the Po Plain

mask at surface the relations between these two chains. Recent study showed that the Alpine and the Apenninic chain may be considered part of a continuous orogenic system derived from the interaction between the European and Adria plates and the intervening oceanic domains (Molli *et al*., 2010).

The Western Alps are an orogenic wedge constituted by continental and oceanic tectonic units derived from the Alpine Tethys oceanic basin and from the two adjoining passive margins. The Western Alps are characterized by a double verging structure in cross-section (see ECORS-CROP profile in Fig. 2; Roure *et al.* 1990; Schmid and Kissling 2000). The Penninic Front and the Canavese Line, two regional tectonic discontinuities with opposite vergence, separate the axial sector of the chain, which include units (Austroalpine, Penninic and ophiolitic nappes) with high-pressure and low temperature metamorphic assemblages (HP/LT), from the external (Helvetic Domain) and internal sectors (South Alpine Domain), devoid of HP/LT metamorphic imprint (Fig. 2a, c).

The northern Apennines are a fold and thrust belt of oceanic Ligurian units and continental low-grade to non-metamorphic units, stacked in N- to NE-verging sheets. To the north-east, foredeep clastic wedges (Macigno, Modino Cervarola and Marnoso Arenacea Formations of the literature) were progressively developed and deformed during the Tertiary north- to northwestward evolution of the Northern Apennines. The external Fronts of the Northern Apennines are currently buried beneath the Quaternary deposits of the Po Plain.

The Tertiary Piedmont Basin is a large episutural basin developed in the internal sector of the Western Alps since the late Eocene. The Upper Eocene-Miocene deposits of this basin rest on both the Alpine metamorphic units, South Alpine units and the Cretaceous to Lower Eocene non metamorphic Ligurian units. The Tertiary Piedmont Basin is constituted by different tectono-stratigraphic domains, characterized by only partially comparable structural and stratigraphic evolution. They are the Torino Hill and Monferrato to the north, separated by the

Rio Freddo Deformation Zone (RFDZ in Fig. 2; Piana and Polino 1995), and the Langhe, Alto Monferrato and Borbera Grue to the south (Biella *et al*., 1997).

Since the Cretaceous, the N-ward motion of the Adria plate caused the consumption of the Ligurian-Piedmont Basin in a south- to south-east directed subduction. This tectonic phase (Late Cretaceous–Paleocene) is related with the juxtaposition of the Alpine units under high- to very high-pressure metamorphic conditions (Coward and Dietrich 1989; Polino *et al.* 1990; Schmid and Kissling 2000). A number of structural studies indicate that the subduction and the early phases of collision (Paleocene-Eocene) and nappe stacking in the Western Alps occurred in a context of N-directed sinistral oblique convergence (Ricou and Siddans 1986; Dewey *et al.* 1989; Schmid and Kissling 2000; Ceriani and Schmid 2004, Ford *et al.* 2006; Handy *et al*., 2010; Dumont *et al.* 2011). The final closure of the Alpine Tethys culminated in the collision and indentation of Adria into Europe (Fig. 2c) in the Late Eocene-Early Oligocene (Tricart 1984; Rosenbaum and Lister 2005). According to some studies, this tectonic phase generated in the Western Alpine chain regional N-S left-lateral regional shear zones (Ricou and Siddand 1986; Ceriani and Schmid 2004) and N-NW verging thrust systems (Dumont *et al*. 2011).

Since the early Oligocene, the Adriatic plate began to move towards WNW causing a strong reworking in the Alpine chain (Coward and Dietrich 1989; Dumont *et al.* 2011). This tectonic phase was related with the development of a complex brittle-ductile to brittle fault network.

In the northern and central sector of the Western Alps the post-collisional tectonics induced dextral strike-slip and dextral-reverse faulting both in the most internal (CL, LTZ, SAF in Fig. 2; Schmid *et al.* 1987; Balestro *et al.* 2009; Perrone *et al.* 2010; 2013) and in the external sectors of the chain (CHL, RL in Fig. 2; Gourlay and Ricou 1983; Hubbard and Mancktelow 1992; Perello *et al.* 2001; Tricart 2004; Baietto *et al.* 2009; Festa *et al.* 2009; Mosca *et al.* 2010; Perello *et al.* 1999; Sommaruga 1999). In the axial part of the chain a complex network

of brittle-ductile to brittle faults showing both normal and transcurrent movements with contrasting kinematic evolution has been described (CFZ; LF; TF; ARL in Fig. 2a; Cannic *et al.* 1999; Bistacchi *et al.* 2000; Rolland *et al.* 2000; Collombet *et al.* 2002; Calais *et al.* 2002; Tallone *et al.* 2002; Agard *et al.* 2003; Sue and Tricart 1999, 2002, 2003; Delacou *et al.* 2004, 2008; Champagnac *et al.* 2004, 2006; Selverstone 2005; Tricart *et al.* 2001, 2004, 2007; Sue *et al.* 2007; Perrone *et al.* 2011b).

In the south-Western Alps and in the Ligurian Alps the post-collisional tectonic phase is strongly influenced by the opening, since the Early Oligocene, of the Liguro-Provençal basin and the counterclockwise rotation of the Corsica-Sardinia block in the wake of the Apenninic subduction. Three main tectonic events were recently described (Maino *et al.* 2013; Federico *et al.*, 2014). The earlier tectonic phase (Early Oligocene) is associated to an extensional regime that would be associated with the beginning of the Tertiary Piedmont Basin deposition and the fast Eocene-Oligocene exhumation of the Voltri Unit (Maffione *et al.* 2008; Vignaroli *et al*. 2008). The progressive oceanization of the Liguro-Provençal basin caused the development of a regional NW-SE sinistral transtensional regional fault zone (Late Oligocene-Early Miocene), bounded by the Villalvernia-Varzi Line and the Stura Fault (VV and SF in Fig. 2). The protracting of this geodynamic framework forced in the Early-Middle Miocene the rotation of the Ligurian Alps and the Tertiary Piedmont Basin, where a regional transpressional tectonic regime established. In the late Miocene-Quaternary(?) a contrasting kinematic evolution is observed in the Ligurian Alps. A NE-SW compression is observed in the western sector of the chain, associated with the N-NE ward translation of the Appenninic Front (PTF in Fig. 2) onto the Adriatic foreland, whereas a NW-SE shortening is observed in the eastern sector (Voltri Unit).

The tectonic scenario of the Tertiary Piedmont Basin seems to be dominated by shortening, especially in its northern sector (Mosca *et al.* 2010). In the Oligocene the evolution of this

area seems to be related with the propagation of SE-verging South-Alpine thrust Fronts (SAF in Fig. 2), in its northern sector, and with the development of a roughly regional E-W shear zone (AXF in Fig. 2) that has juxtaposed the Alpine metamorphic units to the non-metamorphic Ligurian Unit. Since the Miocene the N-verging thrust fronts (PTF in Fig. 2) propagated toward the North, strongly influencing the tectono-sedimentary evolution of the Tertiary Piedmont Basin.

Figure 2 here

2.2 The inner Graian Alps

In the inner Graian Alps both continental, represented by the Gran Paradiso Unit and by the Sesia-Lanzo Zone, and oceanic units, corresponding to the Lower Susa–Lanzo Valleys Unit (SLU), are present (Fig. 2b).

The Gran Paradiso Unit and the Sesia-Lanzo Zone are interpreted as tectonic slices belonging to the Paleo-European and Paleo-Adriatic margin respectively (Schmid 2004).

The Lower Susa–Lanzo Valleys Unit (SLU) (Fig. 2b and d; Pognante 1980; Cadoppi *et al.* 2002; Balestro *et al.* 2009) corresponds to an eclogitic unit composed of meta-ophiolites and minor metasediments, showing a pervasive re-equilibration under greenschist facies metamorphic conditions (Nicolas 1966, 1974; Pognante 1980; Lagabrielle *et al.* 1989; Pellettier and Muntener 2006). In the easternmost sector of this unit a wide lithological complex, in the literature known as Lanzo Ultramafic Complex (LC), crops out (Piccardo *et al.* 2004 with references).

The LC (Fig. 2b) corresponds to a 150 km^2 wide body of tectonitic peridotites intruded by gabbroic and basaltic dikes. This complex is composed of three main bodies, interpreted as slices of ancient sub-continental litospheric mantle (northern and central bodies) and

astenospheric mantle (southern body), that are separated by two NW-SE sub-vertical shear zones (Boudier 1978; Kaczmarek and Müntener 2008). These shear zones have been recently interpreted as extensional mantle detachment faults that were rotated during the Alpine tectonic evolution (Kaczmarek and Tommasi 2011). The peridotites are bounded by a thick belt of serpentinites that resulted from ocean floor alterations and Alpine metamorphism (Pellettier and Müntener 2006; Debret *et al.* 2013). Eclogite facies metamorphic assemblage (Kienast and Pognante 1988; Pellettier and Müntener 2006; Sandrone and Compagnoni 1977) indicates that the Lanzo Ultramafic Complex underwent Alpine high-pressure metamorphism.

The structural relation between the SLU and LC has been investigated by several studies, which have led to different conclusions. According to the earliest studies (Nicolas 1966, 1974; Nicolas *et al*. 1972) the LC was thought to be separated from the SLU by a regional N-S sinistral transpressive, steeply dipping ductile shear zone, named the Viù-Locana Zone. In this interpretation, the Viù-Locana Zone would correspond to a wide tectonic melange zone, constituted by calcschists with minor slices of meta-ophiolites and albite gneisses and micaschists, which were thought to mark the eastern boundary of the Mesozoic ophiolites. The Viù-Locana Zone was considered one of the most important sinistral discontinuities that drove the earliest tectonic phases of the Western Alps (Boudier 1978 and Ricou and Siddans 1986). By contrast, on the basis of lithostratigraphic and petrologic data, Lagabrielle *et al.* (1989) and Pellettier and Muntener (2006) proposed a primary contact between the LC and the adjoining metasediments outcropping to the west of this unit. In particular, Pellettier and Müntener (2006) suggested that this area could represent a preserved Ocean-Continent Transition Zone of the Alpine Tethys.

More recently, some structural studies (Balestro *et al.* 2009; Perrone *et al.* 2010) showed that the western boundary of the LC is affected by a late- to post-metamorphic deformation zone, up to some kilometres wide, known as the Col del Lis-Trana Deformation Zone (LTZ). The

LTZ extends for 35 km juxtaposing the LC to the SLU and to the Dora-Maira Unit (Fig. 2), a slice of Paleo-European continental crust (Michard *et al.* 1996; Lemoine *et al.* 2000).

The LTZ shows a polyphasic kinematic evolution characterized by an earlier dextral-reverse activity, which caused a progressive steepening and the clockwise rotation of the pre-existing syn-metamorphic structures and the lithological contacts upon approaching from the west to the LTZ. Its activity progressively changed to normal/transtensional movements (Balestro *et al.* 2009). The comparison between fault rocks and available zircon and apatite fission tracks data (see Perrone *et al.*, 2010; 2011a) indicates that the earlier transpressive activity lasted from the Upper Oligocene to the Early Miocene, whereas the subsequent normal movement started from the Early (?) Miocene. Geological and seismological data indicate that the LTZ could be related to the seismicity that affects the inner Western Alps (Perrone *et al.* 2010). Moreover, interferometric, seismological and geomorphologic data suggest that east of the LC, beneath the Plio-Quaternary deposits of the western Po Plain, another possibly active reverse to transpressional fault, named Cottian Alps Border Fault (CABF in Fig. 2a), is present (Perrone *et al.* 2013). These data imply that the LC is bounded by two sub-parallel N-S transpressional brittle structures, the LTZ and the Cottian Alps Border Fault, that seem to have driven the last phases of its exhumation. These structures could form in cross-section a wide flower structure (Perrone *et al.* 2013).

Regional-scale tectonic reconstructions (Mosca *et al.* 2010), moreover, suggest that the late-metamorphic mylonitic zone of the Canavese Line (Schmid *et al.* 1987, 1989) probably extend to the south, beneath the Po Plain, to bound the Graian Alps (Fig. 2).

2.3. The study area

The study area (Fig. 3) includes the northwesternmost part of the contact between the SLU and the LC (Lower Viù valley, inner Graian Alps).

The SLU is represented by a portion of oceanic crust with its related meta-sedimentary cover. The oceanic crust mainly consists of metabasites with minor serpentinites and chlorite-schists (Fig. 3, 4). Metabasites are usually represented by massive and layered meta-basalts with minor meta-gabbros which, locally, display well- preserved magmatic texture. Thin chlorite-schist levels form minor shear zones within the metabasites. The metasedimentary cover is represented by a thin level of albite-chlorite, epidote schists, followed by quartz-micaschists intimately associated with calcschists and by a block in matrix association up to 300-500 metres thick. This association is composed of phyllitic-carbonatic micaschists that include decimetre- to hectometre-scale blocks of marbles, calcschists, metabasites, serpentinites and a few meta-ophicarbonates, albite-rich micaschists, albite-chlorite-epidote-amphibole bearing gneisses and leucocratic gneisses (occasionally with relics of K-feldspar). With the exception of the serpentinites, these blocks usually show transitional and gradational passages to the enveloping phyllitic micaschists, suggesting a sedimentary origin, rather than a tectonic origin as proposed by previous studies (Nicolas 1966, 1969). Only along the contact with the LC, the serpentinite and metabasite blocks sometimes show millimetre-to centimetre-thick levels of chlorite-schists.

The LC almost entirely consists of serpentinites and mylonitic-serpentinites, with minor rodingitized dykes and chlorite-schists.

Figure 3 here

Detailed field mapping has shown that the contact between the LC and the SLU is marked by both a continuous level of chlorite-schists with a strong mylonitic fabric (Fig. 5h), up to some metres thick, and mylonitic serpentinites, which suggests a tectonic coupling for these units. This interpretation is also supported by the different Alpine metamorphic peak recorded by

these units (Pellettier and Müntener 2006). The results of this study also display that this mylonitic contact is displaced and reactivated by several km-long N-S and NW-SE faults that define a brittle-ductile to brittle deformation zone, up to 1500-1600 metres wide. This deformation zone, named Viù Deformation Zone (VDZ hereafter), represents the most prominent structural feature of the studied sector and will be analyzed in detail in the following sections.

The syn-metamorphic structural evolution is characterized by the overprinting of four (D_1 to D_4) ductile deformation phases. The first two deformation phases (D_1 and D_2) occurred under eclogite and blueschist facies metamorphic conditions, whereas the D_3 and D_4 deformation phases occurred under greenschist to late-metamorphic conditions (Nicolas 1974; Pognante 1980; Spalla *et al.* 1983).

The earliest structural features are represented by a transposition schistosity, named S_1, which represents the axial surfaces of centimetre-scale, at times rootless, intrafolial and isoclinal folds. D_1 folds, usually characterized by thickened hinges and thinned limbs, are mainly observed in the more competent albite-rich micaschists, but are scarcely preserved in the pervasively foliated phyllitic micaschists and in the mylonitic serpentinites (Fig. 5a).

The D_2 deformation phase produced a S_2 schistosity, well developed in all the lithologies. S_2 is the axial plane of isoclinal-to-tight folds, ranging from the millimetre-to-hectometre-scale. These structures are usually characterized at the mesoscopic scale by similar profiles, with thickened hinge zones and thinned limbs (Fig. 5a, b, and f). Occasionally, eye-shaped profiles are also observed (Fig. 5c). A type 3 fold interference pattern (*sensu* Ramsay and Huber 1987) is usually produced by the superposition of D_1 and D_2 folds (Fig. 5a). Due to the transposition nature of D_1 and D_2 phases, both in the LC and the SLU, the S_1 schistosity, with the exception of the hinge zone of the D_2 folds, is often transposed into parallelism with the S_2 schistosity, forming a composed S_1/S_2 schistosity, named S_T. As the contact between the LC

and the SLU is parallel to the S_T the juxtaposition between these two units must be considered as being at least as syn-D_2 phase.

Figure 4 here

The third deformation phase (D_3) is less intense compared to D_1 and D_2, and is generally characterized by open-to-close parallel folds (Fig. 5d, e, f) and sometimes by chevron-type folds. A spaced crenulation cleavage, occasionally developed in the micaschists, is associated with the D_3 folds. In the entire study area, the superposition of D_2 and D_3 folds produces, at different scales, a type 3 interference pattern (*sensu* Ramsay and Huber 1987; Fig. 5f).

The D_4 phase is usually observed at the mesoscopic scale and is represented by open folds sometimes showing kink geometry. Gentle-to-open folds with rounded hinge zones are dominant in the micaschist, whilst kink folds dominate in the mylonitic serpentinites of the Lanzo Ultramafic Complex. Usually these folds are characterized by fractures along their axial surface, indicating that they were formed under brittle-ductile conditions (Fig. 5g). The superposition of D_3 and D_4 folds (Fig. 5e) produces, at different scales, a type 1 interference pattern (*sensu* Ramsay and Huber 1987).

Figure 5 here

3. The Viù Deformation Zone

3.1 Methodology

The late to post-metamorphic structural evolution is related to the development of a complex network of faults.

Faults were characterized in the field on the basis of their geometry, kinematics, mineralizations on fault surfaces and fault rocks (Rossetti *et al.* 2002; Perello *et al.* 2004; Perrone *et al.* 2011a; Fusetti *et al.* 2012). Major and minor faults were differentiated on the basis of the length and width of their damage zone. In order to gain a better insight into their geometry and extension, the mapped faults were compared with the morpho-structural elements detected from the aerial photo analysis at a 1:25,000 scale (Fig. 6).

Due to the lack of Neogene geological markers allowing to constrain the age of brittle structures in the field, the relative chronology of late- to post-metamorphic deformation events was based on the analysis of fault rocks, mineralizations along fault surfaces and on overprinting relations between different kinematic indicators.

Sense of shear indicators were mainly obtained by the measurement of S-C structures, Riedel shears, dragged foliations along the fault plane, and by antigorite, chlorite and rare quartz slickensides.

As the possibility that the reactivation of inherited anisotropies, which causes the development of structures at angles different from those predicted by the Coulomb failure criterion (Harris and Cobbold 1984; Flodin and Aydin 2004), the mechanical interaction among different faults (Dupin *et al.* 1993; Pollard *et al.* 1993; Nieto-Samaniego 1999) and the rotation of fault bounded blocks could occur, the analysis of fault-slip data has been carried out using the kinematic approach (Marrett and Allmendinger 1990).

Because the map-scale faults may be regarded as domains of roughly homogeneous brittle deformation, the kinematic analysis is discussed by integrating fault-slip data collected in selected structural stations with single measurements collected along each map-scale fault. An average kinematic solution is then calculated using linked Bingham distribution statistics for each map-scale fault. This approach has allowed us to determine the orientation of the principal axes of the incremental strain ellipsoid, the bulk kinematics of each fault and the

establishment of kinematic compatibility between different faults (see also Claypool *et al.* 2002; Perrone *et al.* 2011a). Only the best quality kinematic indicators were used in this study.

Figure 6 here

3.2. Brittle deformation inside the VDZ

The most important late- to post-metamorphic structural feature is represented by the Viù Deformation Zone (VDZ). It extends in N-S direction and affects the central-eastern sector of the study area, displacing the contact between LC and SLU. Approaching from the west the VDZ the S_T, usually moderately dipping to the NE in the SLU, becomes progressively steeper and tends to rotate towards N-S direction. Inside the VDZ, S_T is sub-vertical and N-S to NW-SE striking, whereas east of the VDZ it is usually steeply dipping both to NW and SE. D_2 and D_3 fold axes and axial surfaces are usually sub-horizontal to moderately dipping in the SLU, whereas in the LC are mainly steeply dipping to sub-vertical. D_4 folds are usually characterized by steep axial surfaces in the SLU whereas in the LC show sub-horizontal axial surfaces (Fig. 3, 4).

Figure 7 here

The VDZ reaches a width of about 1.5 km and is composed of several N-S steep faults linked by minor NW-SE faults (Fig. 3, 4) that, at map-scale, define a roughly anastomosed geometric pattern. Striae on fault surfaces indicate both strike- and dip-slip movements (Fig. 7).

Major N-S faults reach multi-kilometric length and are usually arranged in a left-stepped en-echelon geometric pattern, especially along the western border of the VDZ (Fig. 3). Due to

the lack of clear geological markers in the entire study area, it was not possible to accurately estimate the amount of displacement. Nevertheless, where possible, the restoration of geological limits indicates a horizontal component of displacement in the order of few hundred metres for each single fault. Morpho-structural analysis (alignment of saddles, streams, slopes and straight valleys and river elbow) also shows that these structures could extend beyond the study area reaching a length of several kilometres (Fig. 6).

Figure 8 here

Figure 9 here

Minor NW-SE faults, usually sub-vertical or steeply dipping both to the NE and SW (Fig. 7), can reach a maximum length of about one kilometre (Fig. 3).

At the mesoscopic scale both N-S and NW-SE faults are usually arranged into steeply dipping damage zones (Fig. 7), up to some tens of metres wide, characterized by N-S to NNE-SSW reverse-dextral and by NW-SE to NNW-SSE sinistral-reverse faults (Fig. 8, 9, 10, 11). In detail, Riedel shears, antigorite and chlorite slickenfibres and dragged foliations indicate reverse, reverse-dextral and subordinate dextral transcurrent movements for the N-S faults (Fig. 8; 9a-d) and sinistral transcurrent to sinistral-reverse and reverse movements for NW-SE faults (Fig. 10a,b; 11a,b,d,e). Anastomosed geometry (Fig. 10a, b), in map-view, and positive flower geometry (Fig. 9a, b; 11b; 12) or conjugate systems (Fig. 8c; 11a), in cross-section, are frequently observed for both N-S and NW-SE faults. When parallel, faults usually reactivate the metamorphic foliation (Fig. 9b; 11d).

Sometimes NE-SW reverse faults with very limited lateral persistence are also found between NW-SE faults (Fig. 11f).

All these faults are usually associated to foliated cataclasites (Fig. 8a, 9b, 10a, b), tectonic breccias, gouges (Fig. 11b, c) and occasionally by $CaCO_3$ cemented-cataclasites, which can reach 20 metres in thickness. The thickness of fault rocks seems to be strictly related to the lithology affected by the brittle deformation. In the homogeneous serpentinites of the LC, the faults are characterized by damage zones and fault cores up to several tens of metres and 20 metres wide, respectively (Fig. 8a; 11c). By contrast, in the pervasively foliated micaschists, brittle shear zones are typically characterized by scarce-to-moderate lateral persistence, by narrow damage zones and are widespread in the whole rock volume.

Sometimes also reverse/transpressional brittle-ductile shear zones have also been observed (Fig. 8b, d; Fig. 11d, e).

Subordinate N-S normal to normal-dextral faults (Fig. 9e, f), mainly associated with tectonic breccias, have been also observed at the mesoscopic scale inside the VDZ. Even if clear overprinting relations between different striae generations have not been found, these faults could be related to a subsequent extensional re(?)-activation of the VDZ, which has been also observed in the adjoining sectors (Balestro *et al.* 2009; Perrone *et al.* 2010, 2011a,b; Fusetti *et al.* 2012).

Figure 10 here

Figure 11 here

3.3 Brittle deformation outside the VDZ

The VDZ separates two low-strained domains affected by discrete faults with very limited length.

West of the VDZ, in the SLU, NW-SE thrust to transpressional faults, up to some tens of metres long, are abundant (Fig. 3). These low-angle to moderately dipping, top to WSW shear zones, well developed especially in the pervasively foliated mica- and chlorite-schists of the SLU, usually drag and reactivate the main schistosity (Fig. 10c, d).

At the mesoscopic scale N-S normal to normal-dextral and NW-SE normal to normal-sinistral faults are also observed in this sector. These structures are characterized by damage zones very limited in thickness (less than 1 metre) and are usually associated with tectonic breccias (Fig. 9e). Rare cross-cutting relations indicate that normal faults postdate reverse/transpressional faults (Fig. 9f).

East of the VDZ, in the serpentinites of the LC, NE-SW faults with very limited lateral persistence are present (Fig. 3). These structures are usually steeply to moderately dipping. Usually, fault rocks are represented by tectonic breccias, up to 1 metre thick, with damage zones that reach a width of a few metres. Very rare kinematic indicators (Riedel shears and antigorite slickenfibres) show normal movements for these structures.

Rarely some E-W faults have been also found at mesoscopic scale (Fig. 7). No reliable kinematic indicators were observed for these structures.

Figure 12 here

3.4 Brittle paleostrain analysis

On the basis of the kinematics, fault-related rocks and cross-cutting relations, two fault populations have been distinguished. In the following description these fault populations will be related to two distinct faulting stages characterised by different orientations of the maximum and minimum incremental shortening axes (P and T axes) and dissimilar fault rocks.

The faulting stage 1 is associated to the development of N-S reverse, transpressional and transcurrent faults, which show similar fault rocks (foliated cataclasites and tectonic breccias), mineralizations (antigorite) on fault surfaces and kinematic indicators.

The reverse to reverse/dextral and subordinate dextral transcurrent movements along the N-S faults are consistent with a sub-horizontal, E-W to ENE trending shortening axis with steeply to moderately dipping extension axis (stations 1, 4, 5, 6, 8, 16, 19, and 20 in Fig. 13). The variability of the component of displacement of these faults is, therefore, interpreted in terms of kinematic partitioning of the transcurrent and reverse component of movement along the VDZ. In particular, reverse to reverse-dextral movements are consistent with a sub-horizontal ENE-WSW to E-W shortening with a moderately to steeply dipping extension, whereas subordinate dextral transcurrent movements are consistent with a sub-horizontal NE-SW shortening and a NW-SE extension axis.

The average kinematic solutions that incorporate all of the data sets for each N-S major fault of the VDZ show reverse and reverse-dextral fault planes that are steeply dipping to the west and to the east in the western and eastern part of this structure respectively (Fig. 14a).

The different reverse to sinistral-reverse and sinistral transcurrent movements found along the minor NW-SE faults (stations 2, 3, 13, 15, and 18 in Fig. 13), which show fault rocks similar to those observed for the N-S transpressional faults, may be, instead, related to block rotation inside the VDZ. Probably, these faults were firstly formed as reverse faults, roughly perpendicular to the VDZ. The protracted activity of the N-S boundary faults caused the clockwise rotation of the blocks inside the VDZ, inducing reverse-sinistral to sinistral movements along these faults (see Fig. 14c). This mechanism was probably controlled by the attitude of the inherited structures, as suggested by the strong similarity between the attitude of the metamorphic schistosity (S_T) and faults in this sector (Fig. 15). The average solution for

the NW-SE fault inside the VDZ shows a sinistral-reverse movement along a sub-vertical NW-SE striking fault plane (Fig. 14a).

The geometry of the VDZ, characterized by lozenge-shaped fault-bounded domains, the opposite dipping of the N-S boundary faults and the transpressional kinematics of the faults associated with this faulting stage indicate that the VDZ can be interpreted as a km-scale positive flower structure displacing the LC and the SLU (Fig. 12, 14a, b). The rare NE-SW striking reverse faults observed inside the VDZ, instead consistent with a NW-SE shortening, represent bridge structures (*sensu* Gamond 1987) developed between sub-parallel NW-SE transcurrent/transpressional faults (station 10 in Fig. 13 and average solution in Fig. 14a).

Figure 13 here

West of the VDZ, in the SLU, this faulting stage is associated with the development of minor NW-SE striking thrust to sinistral-reverse faults, consistent with a WSW dipping shortening direction (Fig. 10c, d, station 14 in Fig. 13).

Fault rocks (foliated cataclasites and subordinately tectonic breccias), kinematic indicators (dragged foliations) and mineralizations on fault surfaces (antigorite and chlorite slickenfibres) indicate that this flower structure was formed under brittle-ductile to brittle structural conditions. Assuming a geothermal gradient of about 30°C/km (Malusà *et al.* 2009), this structural association may have formed at depth ranging from 4-5 to 10 km (Sibson 1977; Scholz 1988).

The faulting stage 2 seems to be mainly related to the development of N-S normal to normal-dextral faults and NW-SE normal to normal-sinistral faults (stations 7, 9, 11, 12, and 17 in Fig. 13 and average solution in Fig. 14a). These faults are mainly widespread in the SLU at the mesoscopic scale. Rare N-S normal faults found inside the VDZ suggest that it could have

been reactivated during this faulting stage (Fig. 14a), even if no clear overprinting relations have been observed. These faults are mostly consistent with a moderate to steeply dipping to the SW shortening with a WNW-ESE to NE-SW extension (Fig. 13). Fault rocks (tectonic breccias) associated to these structures indicate that this faulting stage occurred under brittle structural conditions, which correspond to 1-4 km depth (Sibson 1977; Scholz 1988).

3.5 Timing constraints for the kinematic evolution of the VDZ

Comparing the different type of fault rocks with the available published (Bernet *et al.* 2001) zircon and apatite fission tracks data (ZFT; Tc=240±30 °C, natural α-damage model of Reiners and Brandon 2006, or Tc=340±40 °C, zero damage model of Brix *et al.* 2002, Rahn *et al.* 2004; AFT; Tc=110±10°C, Reiners and Brandon 2006) it is possible to provide a timing constrain for the two faulting stages. According to the two proposed models, the closure temperature of the ZFT, with a geothermal gradient of 30°C/km, may correspond to depth ranging between 7 and 12 km. The closure temperature of the AFT, instead, corresponds to depth of 3-4 km. In the light of the aforementioned assumptions, as ZFT and AFT show ages ranging between 33 and 30 Ma and 21-18 Ma respectively (see Fig. 2b), these data indicate that this sector of the Western Alps reached a depth compatible with the development of cataclasites (4-10 km depth, Sibson 1977; Scholz 1988), since the Late(?) Oligocene times. Deformation conditions roughly compatible with the development of tectonic breccias (1-3 km depth, Sibson 1997; Scholz 1988), were reached in the Early Miocene. This imply that the faulting stage 1 and may have occurred in the Late(?) Oligocene–Early Miocene and that the faulting stage 2 may be considered as post–early Miocene.

Figure 14 here

4. Discussion

In the following sections we discuss the role played by the VDZ in modifying the pre-existing tectonic setting, its control on the last phases of the exhumation of the metamorphic units and, as a consequence, the geodynamics of the Western Alpine chain. Moreover, the role of the inherited structures on the development and geometry of the VDZ will be considered.

4.1. The role of the Viù Deformation Zone in modifying the pre-existing syn-metamorphic tectonic setting and last stages of exhumation of the metamorphic units

The VDZ has strongly modified the pre-existing structural setting. It bounds and separates, in fact, structurally homogeneous domains (I-V in Fig. 15) characterized by different orientations of the syn-metamorphic structures (S_T, D_2, D_3 and D_4 folds), and by different intensity of brittle deformation. A progressive steepening of the lithological contacts and syn-metamorphic features (S_T, D2 and D_3 fold axes) is observed from west to east in the study area (Fig. 3, 4, and 15). Indeed S_T, which moderately dips to the north-east in the structural domain I, becomes steeply dipping inside (structural domain II, III, IV in Fig. 15) and east (structural domain V in Fig. 15) of the VDZ. D_2 and D_3 fold axes, which are sub-horizontal to moderately plunging from NW-SE to N-S in the structural domain I-II-III, become sub-vertical in the structural domain IV and V. By contrast, the D_4 folds axial surfaces, which are sub-vertical in the structural domain I, become sub-horizontal in the structural domain IV and V.

Figure 15 here

The steepening of the syn-metamorphic structural features seems to be consistent with a rotation induced by the reverse-dextral activity of the VDZ. In the simplified sketch of Figure 16, an attempt to reconstruct the different stages that characterize the transpressional activity of the VDZ, and that drove the last stages of the exhumation of the LC and SLU, is shown. In this model, the LC is assumed to overlay the SLU (Fig. 16a), since west of the study area (see Fig. 2b), several meta-peridotites bodies are usually found at the top of the SLU, as also indicated by Nicolas (1966). The earliest phases of the VDZ activity (Fig. 16b) caused the steepening of the pre-existing lithological contacts and syn-metamorphic structures (S_T and D_1 to D_4 structures) in the eastern part of the study area (structural domains IV and V in Fig. 15; see also Fig. 16b and Fig.16b1 to 16b4). The subsequent, or possibly contemporaneous, development of the N-S faults induced the brittle reactivation, where favourably oriented, and the displacement of the steepened limbs of the D_1 to D_4 folds and of the contact between the LC and the SLU of at least some hundred metres (Fig. 16c). As the deformation proceeded, the sub-parallel N-S reverse-dextral faults, arranged in an en-echelon geometric pattern, were gradually linked by reverse faults sub-perpendicular to the VDZ, forming a km-scale positive flower structure in cross-section (Fig. 16c-e).

The transcurrent component of displacement along the N-S boundary faults caused the dragging and clockwise rotation, on the horizontal plane, of the S_T and the syn-metamorphic structures, which had an increasing effect approaching the VDZ (Fig. 16f, g). In fact, as also observed along the LTZ (Balestro *et al.* 2009) south of the study area, the strike of the main schistosity (S_T) progressively changes from NW-SE (structural domain I; Fig. 15), west of this shear zone, to N-S, inside the shear zone (structural domains II and IV; Fig. 15). Clockwise block rotation could have also occurred within the VDZ, inducing a strong sinistral component of movement along the NW-SE transpressional faults (Fig. 14c, 16f, and g).

The complex pattern of metamorphic schistosity in the LC may be therefore interpreted as the result of both the steepening of D_1 to D_4 folds and of the rotations of fault bounded blocks in the horizontal plane.

The protracted activity of the VDZ caused the exhumation of the SLU with respect to the LC. This is also suggested by the younger ZFT ages (30-33Ma) shown by the SLU with respect to the LC (33Ma; see Fig. 2b). The extensional reactivation of the VDZ probably has caused a slight reworking of the pre-existing contacts, whose amount is difficult to assess only on the basis of the field data.

Figure 16 here

4.2. The VDZ in the frame of the post-Oligocene tectonic evolution of the Western Alps and adjoining domains

Recent studies have shown that a N-S polyphasic, brittle-ductile to brittle structure, named Col del Lis-Trana Deformation Zone (LTZ; Balestro *et al.* 2009; Perrone *et al.* 2010), affects the western border of the LC south of the study area (Fig. 2). The LTZ shows kinematic evolution similar to the VDZ. Its activity (Fig. 17), in fact, evolved from dextral-reverse (Late Oligocene-Early Miocene to normal/transtensional (post-Early Miocene). This allows extending the LTZ further to the north, so that it affects the entire western border of the LC.

In this interpretation the VDZ corresponds to a contractional step-over zone along the LTZ. This explains the strong reverse component of displacement observed along the faults in the study area and the slight discrepancy between the shortening direction observed along the LTZ and the VDZ (Fig. 17b).

The kinematic evolution of the LTZ-VDZ represents a further constrain to the understanding of the post-Oligocene tectonics of the Western Alps. Different models, in fact, have been

proposed to explain the complex tectonic setting of the chain and, hence, its strongly curvilinear shape. The most important include the westward extrusion (Coward and Dietrich 1989; Ford *et al.*, 2006; Dumont *et al.*, 2011, 2012), westward shift of the Alpine front since the Oligocene induced by the retreat of the Apenninic slab (Vignaroli *et al.* 2008), dextral transcurrence at the scale of the chain induced by the counter-clockwise rotation of the Adria plate since Oligocene (Vanossi *et al*. 1994; Castellarin 2001; Collombet *et al.* 2002; Agard *et al.* 2003; Sue and Tricart 2003; Malusà *et al.* 2005, 2009), and polyphasic models that associate south-westward extrusion (Sue *et al.* 2007; Champagnac *et al.* 2004, 2006) or dextral transcurrence combined with buoyancy forces (Delacou *et al.* 2004; Perello *et al.* 2004; Perrone *et al.* 2011a).

The kinematic evolution of the LTZ fits well in a model where the WNW-ward propagation (with the subsequent indentation), coupled with counter-clockwise rotation, of the Adria plate induced a complex partitioning in time and space of the bulk regional deformation that affected the Western Alps since the late Oligocene (Fig. 17; see also Perrone *et al.* 2011).

This indentation is clearly reflected in the propagation of compressive/transpressional faults both in the external domains (Helvetic-Dauphinois cover and basement units in Late Oligocene-early Miocene, Jura belt in middle and late Miocene; Sommaruga 1999; Schmid and Kissling 2000; Ford *et al.*, 2006; Dumont et *al*., 2011; 2012) and in the internal domains (Late Oligocene, Southern Alpine Thrusts; Festa *et al.* 2009; Mosca *et al.* 2010) of the northern and central sector of the Western Alps (Pennine, Graian, Cottian and western Maritime Alps).

It is, therefore, very likely that the WNW-ESE convergence between Adria and Europe should have been increasingly recorded moving from the axial part of the chain, mostly affected by transcurrent and transtensional faulting, to its margins (both internal and external), where

thrust to transpressional tectonics is developed (Sue and Tricart 2003; Delacou *et al.* 2004; Perrone *et al.* 2011a).

In this scenario a strain partitioning process, in which some faults accommodated the indentation and some others the rotational component, may be plausible.

Some of the regional fault systems, like the Southern Alpine Thrusts beneath the Po Plain (SAF in Fig. 2a, 29 and 30 in Fig. 17a; Late Oligocene; Mosca *et al.* 2009) the Penninic Front (PF in Fig. 2a; see 3 in Fig. 17a; Perello *et al.* 1999), the roughly W-verging thrusts in the Helvetic Domain (Early Miocene?; Sommaruga 1999) and in the Pelvoux area (Oligocene; 28 in Fig. 17a; Dumont *et al.* 2011, 2012), and the E-W dextral transcurrent faults displacing the Gran Paradiso Unit (OSZ in Fig. 2a; 2 in Fig. 17a; Perello *et al.* 2004) and the Sesia-Lanzo Unit (23 in Fig. 17a; Fusetti *et al.* 2012) accommodated the NW-SE regional shortening.

At the same time (Oligocene?- Early Miocene?) the dextral transcurrent and transtensional regional faults accommodated both the anticlockwise rotation of the Adria plate and the (minor) gravitational body forces active inside the more elevated part of the chain. In particular the rotational component were accommodated by the dextral movements along the Chamonix-Rhone Line, the Rhone Line (CHL and RL in Fig. 2a; Gourlay and Ricou 1983), the NW-SE faults affecting the Argentera Massif (9 in Fig. 17a; Perello *et al.* 1999; Tricart 2004; Baietto *et al.* 2009) and by the dextral activity along the LTZ (faulting stage 1 in this study), the Colle delle Finestre Deformation Zone (CFZ in Fig. 2a; 31 in Fig. 17a; Tallone *et al.* 2002; Perrone *et al.* 2011a) and the Canavese Line (CL in Fig. 2a; Schmid *et al.* 1989). The early normal activity of the Longitudinal and Transversal Faults (LF and TF in Fig. 2a; 7 and 12 in Fig. 17a) displacing the Briançonnais units and the extensional regime observed in the Aosta and in the Valais area (1, 11, 22, in Fig. 17a; Champagnac *et al.* 2004, 2006) could be, instead, related to body forces already active inside the chain (see Sue and Tricart 2003; Delacou *et al.* 2004; Perrone *et al.* 2011a, b).

In the same period in the south-Western Alps (eastern Maritime and Ligurian Alps) and in the southern sector of the Tertiary Piedmont Basin the coeval progressive opening of the Balearic rift and the counter-clockwise rotation of the Corsica-Sardinia block in the rear of the Apenninic subduction caused in the earliest phases (Early Oligocene; Vignaroli *et al.* 2008; Maino *et al.* 2012, 2013; Festa *et al.* 2015) the development of an extensional regime and, later (Late Oligocene) the development of a roughly WNW-ESE left-lateral regional fault zone (25 in Fig. 17a; Maino *et al.* 2013). At this time the Villavernia-Varzi Line (27 in Fig. 17a; Festa *et al.* 2015) and the Stura Line acted as sinistral faults whereas the Sestri-Voltaggio Line was characterized by antithetical right-lateral movements (24 in Fig. 17a; Capponi *et al.* 2009; Federico *et al.* 2014). In the early Miocene the Corsica-Sardinia block accomplished their counter-clockwise rotation of 50° inducing a comparable rotation in the Ligurian Alps-Tertiary Piedmont Basin which was affected by transpression (Maino *et al.* 2013).

In the northern sector of the Tertiary Piedmont Basin the Oligo-Early Miocene tectonic evolution is mostly related, as well as with the propagation of the South-Alpine thrusts (29 and 30 in Fig. 17a; Festa *et al.*, 2009; Mosca *et al.* 2010), with the sinistral transpressive movements along the Rio-Freddo Deformation Zone (26 in Fig. 17a; Piana 2000).

Starting from the Early Miocene(?) the convergence rate between the two colliding plates was progressively reduced and the gravitational body forces became dominant on the rotational movements in the inner Western Alps (Fig. 17d, e), where a extensional regime was established (Champagnac 2004, 2006; Sue *et al.* 2007; Malusà *et al.* 2009; Perrone *et al.* 2011a). This progressive change of stress regime caused the gradual transition or the normal/transtensional reactivation (faulting stage 2 in this study) of the faults affecting the axial part of the chain, including the faults affecting the Cottian and Graian Alps (like the LTZ, CFZ, OSZ in Fig. 2a; 2, 5, 6, 31 in Fig. 17d; Tallone *et al.* 2002; Perello *et al.* 2004; Balestro *et al*. 2009) and the Aosta and Valais areas (1, 13, 15 in Fig. 17d; Champagnac *et al.*

2004; 2006). Only the structures affecting the units of the Briançon and Queyras areas and the Argentera Unit (7, 8, 9 and 33 in Fig. 17d) are active as dextral transcurrent faults during this phase (Sue and Tricart 2003; Perello *et al.* 1999; Baietto *et al.* 2009; Sanchez *et al.* 2010; Bauve *et al.* 2014). In the study area the change from the first faulting stage to the second caused the permutation between the maximum and minimum shortening axes relative to the two faulting stages, which are roughly E-W striking (Fig. 17c and f). This extensional tectonic regime is still ongoing in the inner Western Alps whereas in the outer borders of the chain a transpressional regime is still dominant, as indicated by the more recent seismotectonic studies (Delacou *et al.* 2004; Sue *et al.* 2007; Perrone *et al.* 2010, 2011b).

By contrast, in the southern sector of the Western Alps (Ligurian Alps) and in the Tertiary Piedmont Basin, the post-Early Miocene tectonic evolution seems to be mostly related to the N-ward propagation of the North-Apenninic Thrust (PTF in Fig. 2; see Mosca *et al*. 2010; Maino et *al.* 2013; Festa et *al.* 2015). Also the Ligurian Sea, since the Pliocene, shortening is undergoing a compressive regime (33 in Fig. 17d; Sage *et al.* 2011; Bauve *et al.* 2014).

In summary, all these data suggest that, since the Oligocene, the tectonic setting of the Western Alps must be primarily considered as the result of the convergence and the counter-clockwise rotation of the Adria plate which induced several coexisting tectonic processes such as the opening of the Provençal and Tyrrhenian basins, the growing of two interfering chains (the Alps and the northern Apennines) and, even if as a consequence, the development of gravitational body forces inside the axial sector of the Western Alps. The concomitance of all these mechanisms strongly influenced the curvilinear shape of the Western Alps, as also proposed by some authors (Maino *et al.* 2013).

Other geodynamic processes proposed for the inner Western Alps, such as the south-ward (Champagnac *et al.* 2004, 2006; Sue *et al.* 2007) or the west-ward extrusion (Coward and

Dietrich 1989; Dumont *et al.* 2011) do not seem to be in agreement with the whole of these kinematic data.

For the south-ward extrusion, in fact, would be necessary two antithetical transcurrent zones, sub-parallel to the trend of the chain, which allow driving this movement. If the dextral transcurrent zone would correspond to the Chamonix-Rhone Line and to the Longitudinal Faults, towards the external sectors, it is still not possible to detect a regional left-lateral zone in the innermost sector of the chain where, by contrast, mostly dextral faults are observed.

The westward extrusion, by contrast, assumes a frontal collision since the Oligocene between the Adriatic and the European plates, which is in contrast with the strong transcurrent component of displacement shown by the faults affecting the inner Western Alps.

Finally, the model proposed by Vignaroli *et al*. (2008), which suggest that the curvilinear shape of the Western Alps was forced since the Oligocene by the opposite retreat of the Apennines and Alpine slabs, inducing a regional extensional regime in the SW and Ligurian Alps, does not fit with the structural and the seismological data, which show a protracted transcurrent/transpressive regime in this area since the Early Miocene (Fig. 17d; Sage *et al.* 2011; Maino *et al.* 2013; Bauve *et al.* 2014; Federico *et al.*, 2014). Malusà *et al.* (2011), in fact, propose a similar mechanism only for the Eocene Western Alps.

Figure 17 here

4.3. Influence of the pre-existing structures on the development and geometry of the VDZ and LTZ

The VDZ shows in map-view a strike-slip duplex geometry that consists of NW-SE sinistral-reverse faults that link left-stepped to sub-parallel N-S reverse-dextral faults. The kinematics of minor connecting faults do not correspond to that classically described in literature for

strike-slip duplex, usually characterized by synthetical faults (Christie-Blick and Biddle 1985; Sylvester 1988; Woodcock and Fischer 1986; Woodcock and Schubert 1994; Woodcock and Rickards 2003). These anomalous geometrical and kinematic relations, although described in the literature as a result of analogue models (see Fig. 17a in Bonora and McClay 2001), yet are poorly described in the field studies (Kim *et al.* 2003; Flodin and Aydin 2004).

The good correspondence between the attitude of the faults and the S_T (Fig. 15c) indicates that the pre-existing anisotropies have strongly controlled the geometry and kinematics of the VDZ.

As previously observed, in fact, the steepening of the syn-metamorphic structures (S_T and D_2-D_4 folds) in the earliest phases of the VDZ probably provided suitably oriented inherited anisotropies for brittle reactivation. As a consequence of this reactivation, the minor faults that connect the N-S faults could have formed under unfavourably attitude with respect to the local shortening and were later clockwise rotated by major faults. Blocks rotation between N-S dextral faults, therefore, induced antithetical sinistral component of movements along the steep NW-SE linking faults (Fig. 14c). This mechanism could, therefore, explain the anomalous geometrical and kinematic relations observed for the VDZ.

Moreover, in cross-section the VDZ shows some similarities with that described by Woodcock and Rickards (2003), characterized by a monocline with a sub-vertical limb displaced by an asymmetric positive flower structure (Fig. 1). In the study area only a part of the monocline, which corresponds to the antiform, can be observed as the whole structure could be buried beneath the deposits of the Po Plain. However some considerations, like the rotation of the NW-SE mantle shear zones that displace the LC (Kazmareck and Tommasi 2011) and the possible presence of other regional reverse/transpressional tectonic features located east of the LC, like the postulated southern prolongation of the mylonitic Canavese Line (Mosca *et al.* 2010; CL in Fig. 2, 18) and/or the Cottian Alps Border Fault (CABF in

Fig. 2, 18) indicate that the whole LC has been steepened by the activity of transpressional syn- and, subsequently, late- and post-metamorphic shear zones. The kinematic and geometric relations between all these faults and the LC suggest that the possible remnants of the adjoining synform could be located east of this unit, beneath the Po Plain, and could have been displaced by the Cottian Alps Border Fault and, probably, by the southern prosecution of the Canavese Line (Fig. 18). The overall geometry defined by the LTZ, the Canavese Line (?) and the Cottian Alps Border Fault could, therefore, resemble the structure described by Woodcock and Rickards (2003). These authors correlate the development of the monocline and the associated positive flower structure to a forced folding induced by the reactivation of a brittle precursor. In the case of the LTZ and the Cottian Alps Border Fault, the reactivated pre-existing discontinuity may be represented by the Ivrea body, which corresponds to a protuberance of the Adriatic mantle intruded beneath (about 7-8 km depth) the inner Western Alps (Fig. 18). The western border of the Ivrea body, which roughly overlaps with the LTZ/VDZ and partially with the Cottian Alps Border Fault, may therefore have induced, starting from the Late Oligocene, the development of the deformations related to the LTZ, first through a forced folding and subsequently, with the progressive exhumation of the chain towards shallower crustal levels, through the development of high-angle transpressional shear zones and faults. The good correspondence between the trace of the western border of the Ivrea body and the LTZ also justifies the length of this transpressional deformation zone and suggests that it could extend southwards to border the south-Western Alps.

Figure 18 here

4.4. LTZ/VDZ versus Viù-Locana Zone

Previous studies proposed that the structural setting of the Graian Alps was largely conditioned by the activity of a regional syn-metamorphic shear zone, known as Viù-Locana Zone (Fig. 18; Nicolas 1966; Nicolas 1974; Boudier 1978). The Viù-Locana Zone developed under HP-LT metamorphic conditions and corresponds to a tectonic mélange zone, up to 1-2 km wide, characterized by slices of meta-ophiolites and gneisses enveloped in a matrix mainly composed of calcschists, which also affects the western border of the LC. According to these studies the steeply plunging folds of D_1 and D_2 phases were formed during the activity of this shear zone. The subsequent D_3 and D_4 folds, characterized by sub-horizontal axes, were not associated to the Viù-Locana Zone and have deformed this ductile shear zone. No impact on the structural setting was related to the post-metamorphic structures.

This study, however, shows that the current structural setting resulted from the rotation around a sub-horizontal axis of all the syn-metamorphic structures (D_1 to D_4) present in the LC and SLU, induced by the transpressional activity of the LTZ/VDZ (Fig. 15, 16). The rotation of the NW-SE shear zones that displace the LC, observed by Kazmareck and Tommasi (2011), is in agreement with this interpretation, suggesting that the entire LC has been rotated around a vertical axis. This rotation may have been driven by the transpressional faults that bound the LC, which correspond to the LTZ and the Cottian Alps Border Fault (Fig. 2 and 18).

The current structural setting of the innermost central sector of the Western Alps seems to have recorded a long tectonic evolution (Fig. 16), in which the post-metamorphic deformation phases have played an important role, rather than being almost entirely associated to earliest phases of its tectonic history. Important near-surface rigid rotations, described farther north (inner Sesia-Lanzo Zone) by Berger *et al.* (2012) also highlight the impact of the last tectonic phases on the structural setting of the inner Western Alps.

5. Conclusions

Different considerations and implications can be drawn from this study.

At the regional scale this paper shows that:

- the northwestern border of the Lanzo Ultramafic Complex is affected by the Viù Deformation Zone (VDZ), a late- to post-metamorphic reverse-dextral structure, which has strongly modified the pre-existing syn-metamorphic structural setting of the area;
- the VDZ is characterized by strike-slip duplexes, defined by N-S reverse-dextral faults linked by NW-SE sinistral-reverse faults, and is interpreted as a km-wide step-over zone of the Col del Lis-Trana Deformation Zone (LTZ), indicating that the western border of the LC is entirely affected by the LTZ;
- the dextral-reverse LTZ probably merges at depth with the Cottian Alps Border Fault, another reverse/transpressional fault buried beneath the western Po Plain, forming an asymmetric positive dextral flower structure that bound the Lanzo Ultramafic Complex, which have caused the rotation around the horizontal plane and driven the exhumation of the Lanzo Ultramafic Complex since the late Oligocene. The development of this structure, which probably slightly postdates the dextral-reverse activity of the mylonitic Canavese Line, may have been controlled by an important buried anisotropy (Ivrea body).
- the kinematics of these N-S regional faults, with a strong dextral component of movement, is consistent with a model of NW-directed convergence combined with an anticlockwise rotation of the Adria plate, as also proposed by recent studies.
- the Viù-Locana Zone, in the light of this reconstruction, considered one of the most important ductile shear zones of the inner Western Alps by previous studies, must be

rather considered a syn-metamorphic tectonic contact between SLU and LC rotated by the activity of the N-S transpressional faults.

More in general, this study indicates that in the metamorphic belts, usually characterized by polyphasic deformations with several inherited anisotropies:

- faulting is strongly controlled by the attitude of the pre-existing structures. In particular, this study shows that the mechanisms that generate strike-slip duplexes may be different from those classically provided by the literature, with brittle reactivation and block rotation strongly prevailing on newly formed faults;

- the occurrence of pre-existing anisotropies seems to have induced kinematic partitioning along the brittle deformation zones, with complex patterns of shortening and extension directions associated to a single faulting stage, especially at the mesoscopic scale. This implies that the kinematic (or dynamic) analysis of fault slip data should not be carried out only on the basis of the attitude of the three main strain (or stress) axes, but further rheological (fault rocks, mineralizations) and timing constraints (AFT and ZFT) must be considered in order to reconstruct the post-metamorphic tectonic evolution of these domains.

- the rotations associated to transpressional faulting may be sometimes mistaken with steep ductile shear zones. The lack of recognition of these brittle deformations and of their consequent rotations may cause misinterpretations in the tectonic reconstructions of such orogens.

Acknowledgments

Andrea Festa is acknowledged for the accurate revision of an earlier version of the paper. We greatly thank Silvio Seno and Enrico Tavarnelli for their very constructive reviews which greatly improved the manuscript.

References

Agard, P., Fournier, M., and Lacombe, O., 2003, Post-nappe extension in the inner Western Alps (Liguro-Piemontese Schistes Lustrés): continuity with late ductile exhumation: Terra Nova, v. 15, p. 306-314.

Allmendinger, R.W., Charlesworth, H.A.K., Earslev, E.A., Guth, P., Langenberg, C.W., and Pecher, A., Whalley, J.S., 1991, Microcomputer software for structural geologists: Journal of Structural Geology, v. 13, p. 1079-1083.

Baietto, A., Perello, P., Cadoppi, P., and Martinotti, G., 2009, Alpine tectonic evolution and thermal water circulations of the Argentera Massif (South-Western Alps): Swiss Journal of Geoscience, v. 102, p. 223-245.

Balestro, G., Cadoppi, P., Perrone G., and Tallone S., 2009, Tectonic evolution along the Col del Lis-Trana deformation Zone (Internal Western Alps): Italian Journal of Geosciences, v. 128, p. 331-339.

Bauve, V., Plateaux, R., Rolland, Y., Sanchez, G., Bethoux, N., Delouis, B. and Darnault, R., 2014, Long-lasting transcurrent tectonics in SW Alps evidenced by Neogene to present-day stress fields, Tectonophysics,doi:10.1016/j.tecto.2014.02.006.

Berger, A., Mercolli, I., Kapferer, N., and Fügenschuh, B., 2012, Single and double exhumation of fault blocks in the internal Sesia-Lanzo Zone and the Ivrea-Verbano Zone (Biella, Italy): International Journal of Earth Sciences, v. 101, p. 1877-1894.

Bernet, M., Zattin, M., Garver, I., Brandon, M.T., and Vance, J., 2001, Steady-state exhumation of the European Alps: Geology, v. 29, p. 35-38.

Béthoux, N., Sue, C., Paul, A., Virieux, J., Fréchet., J., Thouvenot., F, and Cattaneo, M., 2007, Local tomography and focal mechanisms in the south-western Alps: comparison of methods and tectonic implications: Tectonophysics, v. 432, p. 1-19.

Biella, G., Polino, R., De Franco, R., Rossi, P.M., Clari, P., Corsi, A.. and Gelati, R., 1997, The crustal structure of the western Po plain: reconstruction from the integrated geological and seismic data: Terra Nova, v. 9, p. 28-31.

Bigi, G., Castellarin, A., Coli, M., Dal Piaz, G.V., Sartori, R., Scandone, P., and Vai, G.B., 1990, Structural Model of Italy, scale 1. 500 000, sheet n. 1: C.N.R., Progetto Finalizzato Geodinamica, Selca Firenze.

Bistacchi, A., Massironi, M., Eva E., and Solarino S., 2000, Miocene to present kinematics of the NW-Alps: evidence from remote sensing, structural analysis, seismotectonics and thermocronology: Journal of Geodynamics, v. 30, p. 205-228.

Bonora, M. and McClay, K., 2001, Analog models of restraining stepovers in strike-slip fault

systems: AAPG Bulletin, v. 85, p. 233-260.

Boudier, F., 1978, Structure and petrology of the Lanzo peridotite massif (Piedmont Alps): Geological Society of American Bulletin, v. 89, p. 1574-1591.

Brix, M.R, Stöckhert, B., Seidel, E., Theye, T., Thomson, S.N., and Küster, M., 2002, Thermobarometric data from a fossil zircon partial annealing zone in high pressure–low temperature rocks of eastern and central Crete, Greece: Tectonophysics, v. 349, p. 309–326.

Cadoppi, P., Castelletto, M., Sacchi, R., Baggio, P., Carraro, F., and Giraud, V., 2002, Note illustrative della Carta Geologica d'Italia, scale 1:50.000, Susa – 154 Sheet: APAT, Rome – Italy, 123 p.

Calais, E., Nocquet, J.M., Jouanne, F., and Tardy, M., 2002, Current strain regime in the Western Alps from continuous Global Positioning System measurements, 1996–2001: Geology, v. 30, p. 651-654.

Cannic, S., Mugnier, J.L., and Lardeaux, J.M., 1999, Neogene extension in the western Alps: Memorie di Scienze Geologiche di Padova, v. 51, p. 33-45.

Capponi, G., Crispini, L, Federico, L., Piazza, M. and Fabbri, B., 2009, Late Alpine tectonics in the Ligurian Alps: Constraints from the Tertiary Piedmont Basin conglomerates: Geological Journal, v. 44, p. 211–244, doi:10.1002/gj.1140.

Castellarin, A., 2001, Alps-Apennines and Po Plain-Frontal Apennines relations, *in* Vai, G.B., Martini, P., eds., Anatomy of an Orogen: the Apennines and adjacent Mediterranean Basins: Kluwer Academic Publishers, Great Britain, p. 177-196.

Ceriani, S., and Schmid, S.M., 2004, From N–S collision to WNW-directed post-collisional thrusting and folding: structural study of the Frontal Penninic Units in Savoie (Western Alps, France): Eclogae Geologicae Helveticae, v. 97, p. 347–369.

Champagnac, J.D., Sue, C., Delacou, and B., Burkhard, M., 2004, Brittle deformation in the inner northwestern Alps: from early orogen-parallel extrusion to late orogen-perpendicular collapse: Terra Nova, v. 16, p. 232-242.

Champagnac, J.D., Sue, C., Delacou, B., Tricart, P., Allanic, C., and Burkhard, M., 2006, Miocene orogen-parallel extension in the inner Western Alps revealed by dynamical fault analyses: Tectonics, v. 25, p. TC3014.

Christie-Blick, and N., Biddle, K.T., 1985, Deformation and basin formation along strike-slip faults, *in* Biddle, K.T., and Christie-Blick, N., eds., Strike-slip Deformation, Basin Formation and Sedimentation: Special Publication of the Society of Economic Paleontologists and Mineralogists, v. 37, p. 1–34.

Claypool, A.L., Klepeis, K.A., Dockrill, B., Clarke, G., Zwingmann, H., and Tulloch, A., 2002, Structures and kinematics of oblique continental convergence in Northern Fiordland, New Zealand: Tectonophysics, v. 359, p. 329-358.

Collombet, M., Thomas, J.C., Chauvin, A., Tricart, P., Bouillin, J.P., and Gratier, J.P., 2002, Counterclockwise rotation of the Western Alps since the Oligocene: new insights from paleomagnetic data: Tectonics, v. 21, p. 278-293.

Coward, M.P., and Dietrich, D., 1989, Alpine tectonics - an overview, *in* Coward, M.P., Dietrich, D., and Park, R.G., eds., Alpine tectonics. London, Geological Society, Special Publications, 45, p. 1-29.

Debret, B., Nicollet, C., Andreani, M., Schwartz, S., and Godard, M., 2013, Three steps of serpentinization in an eclogitized oceanic serpentinization front (Lanzo Massif – Western Alps): Journal of Metamorphic Geology, v. 31, p. 165–186.

Delacou, B., Sue, C., Champagnac, J.D., and Burkhard, M., 2004, Present–day geodynamics in the bend of the western and central Alps as constrained by earthquake analysis: Geophysical Journal International, v. 158, p. 753-774.

Delacou, B., Sue, C., Nocquet, J.M., Champagnac, J.D., Allanic, C., and Burkhard, M. 2008, Quantification of strain rate in the Western Alps using geodesy: comparisons with seismotectonics: Swiss Journal of Geosciences, v. 101, p. 377-385.

Dewey, J.F., Helman, M.L., Turco, E., Hutton, D.H.W., and Knott, S.D., 1989, Kinematics of the western Mediterranean, *in* Coward, M.P., Dietrich, D., and Park R.G. eds., Alpine Tectonics: London, Geological Society, Special Publications, vol. 45, p. 265-283.

Dewey, J.F., Holdsworth, R.E., and Strachan, R.A., 1998, Transpression and transtension zones, *in* Holdsworth, R.E., Strachan, R.A., and Dewey, J.F., eds., Continental Transpressional and Transtensional Tectonics: London, Geological Society, Special Publication, v. 135, p. 1–14.

Dumont, T., Simon-Labric, T., Authemayou, C., and Heymes, T., 2011, Lateral termination of the north-directed Alpine orogeny and onset of westward escape in the Western Alpine arc: Structural and sedimentary evidence from the external zone: Tectonics, v. 30, TC5006, doi:10.1029/2010TC002836.

Dumont, T., Schwartz, S., Guillot, S., Simon-Labric, T., Tricart, P., Jourdan, S., 2012, Structural and sedimentary records of the Oligocene revolution in the Western Alpine arc: Journal of Geodynamics 56-57, 18–38.

Dupin, J.M., Sassi, W., and Angelier, J., 1993, Homogeneous stress hypothesis and actual fault slip: a distinct element analysis: Journal of Structural Geology, v. 15, p. 1033–1043.

Eva, E., Solarino, S., Eva, and C., Neri, G., 1997, Stress tensor orientation derived from fault plane solution in the Southwestern Alps: Journal of Geophysical Research, v. 102, p. 8171-8185.

Federico, L., Crispini, L., Vigo, A., and Capponi, G., 2014, Unravelling polyphase brittle tectonics through multi-software fault-slip analysis: The case of the Voltri Unit, Western Alps (Italy): Journal of Structural Geology, v. 68, p. 175-193.

Festa, A., Dela Pierre, F., Irace, A., Piana, F., Fioraso, G., Lucchesi, S., Boano, P., and Forno, M.G., 2009, Note illustrative della Carta Geologica d'Italia, scale 1:50.000, 156 sheet - Torino Est: ISPRA – Rome, Italy, 143 p.

Festa, A., Fioraso, G., Bissacca, E. and Petrizzo, M.R., 2015, Geology of the Villalvernia – Varzi Line between Scrivia and Curone valleys (NW Italy): Journal of Maps, v. 11, p. 39-55.

Flodin, E.A., and Aydin, A., 2004, Evolution of a strike-slip fault network, Valley of Fire State Park, southern Nevada: Geological Society of America Bulletin, v. 116, p. 42-59.

Ford, M., W. H. Lickorish, and N. J. Kusznir (1999), Tertiary foreland sedimentation in the Southern Subalpine Chains, SE France: A geodynamic appraisal: Basin Research, 11, 315–336.

Ford, M., Duchene, S., Gasquet, D., and Vanderhaeghe, O., 2006, Two-phases orogenic convergence in the external and internal Alps: Journal of Geological Society of London, v. 163, p. 815–826.

Fusetti, E., Perrone, G., Morelli, M., and Cadoppi, P., 2012, Analysis of the fault pattern in the lower Lanzo valley: an integrated approach: Italian Journal of Geosciences, v. 131, p. 286-301.

Gamond, J.F., 1987, Bridge structures as sense of displacement criteria in brittle fault zones: Journal of Structural Geology, v. 9, p. 609-620.

Goldfinger, C., Kulm, L. D., Yeats, R. S., McNeill, L., and Hummon, C., 1997, Oblique strike-slip faulting of the central Cascadia submarine forearc: Journal of Geophysical Research, vol. 102, p. 8217-8243.

Goodwin, L.B., and Williams, P.F., 1996, Deformation path partitioning within a transpressive shear zone, Marble Cove, Newfoundland: Journal of Structural Geology, v. 18, p. 975–990.

Gourlay, P., and Ricou, L.E., 1983, Le décrochement dextre tardif de la structure de Chamonix (Alpes françaises et suisses): Comptes Rendus de l'Academie des Sciences de Paris - Series IIA - Earth and Planetary Science, v. 296, p. 927–932.

Handy, M., Schmid, S.M., Bousquet, R., Kissling, E. and Bernouilli, D., 2010, Reconciling plate-tectonic reconstructions of Alpine Tethys with the geological–geophysical record of spreading and subduction in the Alps: Earth Science Review, v. 102, 121–158.

Harding, T. P., 1985, Seismic characteristics and identification of negative flower structures, positive flower structures, and positive structural inversion: AAPG Bulletin, v. 69, p. 582–600.

Harland, W. B., 1971, Tectonic transpression in Caledonian Spitzbergen: Geological Magazine, v. 108, p. 27-42.

Harris, L.B, and Cobbold, P.R, 1984, Development of conjugate shear bands during bulk simple shearing: Journal of Structural Geology, v. 7, p. 37-44.

Holdsworth, R.E., Tavarnelli, E., Clegg, P., Pinheiro, R.V.L., Jones, R.R., and McCaffrey, K.J.W., 2002a, Domainal deformation patterns and strain partitioning during transpression: an example from the Southern Uplands terrane, Scotland: Journal Geological Society of London, v. 159, p. 401–415.

Holdsworth, R.,E., Tavarnelli, E., and Clegg., P., 2002b, The nature and regional significance of structures in the Gala Group of the Southern Uplands Terrane, Berwickshire coast, southeastern Scotland: Geological Magazine, v. 139, p. 707-717.

Hubbard, M., and Mancktelow, N.S., 1992, Lateral displacement during Neogene convergence in the Western and Central Alps: Geology, v. 20, p. 943-946.

Jezek, J., Schulmann, K., and Thompson, A.B., 2002, Strain partitioning in front of an obliquely convergent indentor, *in* Bertotti, G., Schulmann, K., and Cloetingh, S.A.P.L., eds., Continental Collision and the tectonosedimentary evolution of forelands: EGU Stephan Mueller Special Publication, Series 1, p. 93–104.

Jiang, D., Lin, S., and Williams, P.F., 2001, Deformation path in high-strain zones, with reference to slip partitioning in transpressional plate boundary regions: Journal of Structural Geology, 23, 991–1005.

Jones, R.R., and Tanner, G.P.W., 1995, Strain partitioning in transpression zones, Journal of Structural Geology, v. 17, p. 793–802.

Jones, R.R., Holdsworth, R.E., Clegg, P., McCaffrey, K., and Tavarnelli, E., 2004, Inclined transpression. Journal of Structural Geology, v. 26, p. 1531–1548.

Kaczmarek, M.A., and Müntener, O., 2008, Juxtaposition of melt impregnation and high temperature shear zones in the upper mantle. Field and petrological constraints from the Lanzo peridotite, (N-Italy): Journal of Petrology, v. 49, p. 2187-2220.

Kaczmarek, M.A., and Tommasi, A., 2011, Anatomy of an extensional shear zone in the mantle (Lanzo massif, Italy): Geochemistry, Geophysics, Geosystems, v. 12, Q0AG06.

Kastrup, U., Zoback, M.L., Deichmann, N., Evans, K., and Giardini, D., 2004, Stress field variations in the Swiss Alps and the northern Alpine foreland derived from inversion of fault plane solutions: Journal of Geophysical Research, v. 109, B01402.

Kienast, J.R., and Pognante, U., 1988, Chloritoid-bearing assemblages in eclogitised metagabbros of the Lanzo peridotite body (western Italian Alps): Lithos, v. 21, p. 1–11.

Kim, Y.S., Peacock, D.C.P., and Sanderson, D.J. 2003, Mesoscale strike-slip faults and damage zones at Marsalforn, Gozo Island, Malta: Journal of Structural Geology, v. 25, p. 793-812.

Labaume, P., Ritz, J.F., and Philip, H., 1989, Failles normales récentes dans les Alpes sud-occidentales: leurs relations avec la tectonique compressive : Comptes rendus de l'Académie des sciences. Série 2, v. 308, p. 1553–1560.

Lagabrielle, Y., Fudral, S., and Kienast, J.R., 1989, La couverture océanique des ultrabasites de Lanzo (Alpes occidentales): arguments lithostratigraphiques et pétrologiques: Geodinamica Acta, v. 3, p. 43-55.

Lardeaux, J.M., Schwartz, S., Tricart, P., Paul, A.,Guillot, S., Béthoux, N., and Masson, F., 2006, A crustal-scale cross-section of the southwestern Alps combining geophysical and geological imagery: Terra Nova, v. 18, p. 412–422.

Lemoine, M., De Graciansky, P.C., and Tricart P., 2000, De l'océan à la chaine de maontagnes, Tectoniques des plaques dans les Alpes: Paris, Gordon and Breach Science Publisher, 207 p.

Lin, S., Jiang, D., and Williams, P.F., 1998, Transpression (or transtension) zones of triclinic symmetry: natural example and theoretical modelling, *in* Holdsworth, R.E., Strachan, R.A., and Dewey, J.F., eds., Continental Transpressional and Transtensional Tectonics: London, Geological Society, Special Publications, v. 135, p. 41–57.

Lu, C.,Y., and Malavieille, J., 1994, Oblique convergence, indentation and rotation tectonic in the Taiwan mountain belt: insights from experimental modeling: Earth and Planetary Science and Letters, v. 121, p. 477–494.

Maffione, M., F. Speranza, C. Faccenna, A. Cascella, G. Vignaroli, and L. Sagnotti 2008, A synchronous Alpine and Corsica–Sardinia rotation, Journal of Geophysical Research, 113, B03104, doi:10.1029/2007JB005214.

Maino, M., Dallagiovanna, G., Dobson, K., Gaggero, L., Persano, C., Seno, S., and Stuart, F.M., 2012, Testing models of orogen exhumation using zircon (U-Th)/He thermochronology: Insight from the Ligurian Alps, Northern Italy: Tectonophysics, v. 560–561, p. 84–93, doi:10.1016/j. tecto.2012.06.045.

Maino, M., Decarlis, A., Felletti, F. and Seno, S., 2013, Tectono-sedimentary evolution of the Tertiary Piedmont Basin (NW Italy) within the Oligo–Miocene central Mediterranean geodynamics: Tectonics, v. 32 (3), p. 593–619. doi:10.1002/tect.20047

Malusà, M.G., Polino, R., Zattin, M., Bigazzi, G., Martin, S., and Piana, F., 2005, Miocene to present differential exhumation in the Western Alps: insights from fission track thermocronology: Tectonics, v. 24, p. TC3004.

Malusà, M.G., Polino, R., and Zattin, M., 2009, Strain partitioning in the axial NW Alps since the Oligocene: Tectonics, v. 28, p. TC3005.

Malusà, M.G., Faccenna, C., Garzanti, E., and Polino, R., 2011, Divergence in subduction zones and exhumation of high pressure rocks (Eocene Western Alps): Earth and Planetary Science and Letters, v. 310, p. 21–32.

Mancktelow, N., 1992, Neogene lateral extension during convergence in the Central Alps: evidence from interrelated faulting and backfolding around the Simplon Pass: Tectonophysics, v. 215, p. 295-317.

Marrett, R., and Allmendinger, R.W., 1990, Kinematic analysis of fault-slip data: Journal of Structural Geology, v. 12, p. 973-986.

Michard, A., Goffé, B., Chopin, C., and Henry, C., 1996, Did the Western Alps develop through an Oman type stage? The geotectonic setting of high-pressure metamorphism in two contrasting Tethyan transects: Eclogae Geologicae Helvetiae, v. 89, p. 43–80.

Molli, G., Crispini, L., Malusà, M., Mosca, P., Piana, F., and Federico, L., 2010, Geology of the Western Alps-Northern Apennine junction area: a regional review, *in*: Beltrando, M., Peccerillo, A., Mattei, M., Conticelli, S., and Doglioni. C., eds., The Geology of Italy: tectonics and life along plate margins: Journal of the Virtual Explorer, v. 36, paper 10, doi:10.3809/jvirtex.2010.00215.

Molnar, P., 1992, Brace–Goetze strength profiles, the partitioning of strike slip and thrust faulting at zones of oblique convergence, and the stress heat flow paradox of the San Andreas Fault, *in* Evans, B., and Wong, T.F., eds., Fault Mechanics and Transport Properties of Rocks: London, Academic Press, p. 435–459.

Mosca, P., Polino, R., Rogledi, S. and Rossi M., 2010, New data for the kinematic interpretation of the Alps-Apennines junction (Northwestern Italy): International Journal of Earth Sciences, v. 99, p. 833-849.

Mount, V.S. and Suppe, J., 1987, State of stress near the San Andreas Fault: implications for wrench tectonics: Geology, v. 15, p. 1143–1146.

Naylor, M. A., Mandl, G., and Sijpesteijn, C. H. K., 1986, Fault geometries in basement-induced wrench faulting under different initial stress states: Journal of Structural Geology, v. 8, p. 737–752.

Nicolas, A., 1966, Étude pétrochimique des Roches vertes et de leurs minéraux entre Dora Maira et Grand Paradis (Alpes piémontaises); le complexe ophiolite-schistes lustres [PhD Thesis]: University of Nantes, 299 p.

____, 1969, Tectonique et métamorphisme dans les Stura di Lanzo (Alpes Piémontaises): Schweizerische Mineralogische und Petrographische Mitteilungen, v. 49, p. 359-377.

____, 1974, Mise en place des péridotites de Lanzo (Alpés Piémontaises): Schweizerische Mineralogische und Petrographische Mitteilungen, v. 46, p. 25-41.

Nicolas, A., Bouchez, J. L., and Boudier, F., 1972, Interprétation cinématique des déformations plastiques dans le massif de lherzolites de Lanzo (Alpes piémontaises). Comparaison avec d'autres massifs: Tectonophysics, v. 14, p. 143-171.

Nieto-Samaniego, A. F., 1999, Stress, strain and fault patterns: Journal of Structural Geology, v. 21, p. 1065–1070.

Oldow, J.S., Bally, A.W., and Ave` Lallemant, H.G., 1990, Transpression, orogenic float and lithospheric balance: Geology, v. 18, p. 991–994.

Paul, A., Cattaneo, M., Thouvenot, F., Spallarossa, D., Béthoux, N., and Fréchet, J., 2001, A three-dimensional crustal velocity model of the south-western Alps from local earthquake tomography: Journal of Geophysical Research, v. 106, p. 19367–19390.

Pelletier, L., and Müntener, O., 2006, High pressure metamorphism of the Lanzo peridotite and its oceanic cover, and some consequences for the Sesia-Lanzo zone (northwestern Italian Alps): Lithos, v. 90, p. 111-130.

Perello, P., Piana, F., Martinotti, G., 1999, Neoalpine structural features at the boundary between the Penninic and Helvetic domains: Eclogae Geologicae Helvetiae, v. 92, p. 347-359.

Perello, P., Marini, L., Martinotti, G., and Hunziker, J.C., 2001, The thermal circuits of the Argentera Massif (western Alps, Italy): An example of low enthalpy geothermal resources controlled by Neogene alpine tectonics: Eclogae Geologicae Helvetiae, v. 94, p. 75–94.

Perello, P., Delle Piane, L., Piana, F., Stella, F., and Damiano, A., 2004, Brittle post-metamorphic tectonics in the Gran Paradiso Massif (North-Western Italian Alps): Geodinamica Acta, v. 17, p. 71-90.

Perrone, G., Eva, E., Solarino, S., Cadoppi, P., Balestro, G., Fioraso, G., and Tallone, S., 2010, Seismotectonic investigations in the inner Cottian Alps: an integrated approach: Tectonophysics, v. 496, p. 1-16.

Perrone, G., Cadoppi, P., Balestro, G., and Tallone, S., 2011a, Post-collisional tectonics in the Northern Cottian Alps (italian Western Alps): International Journal of Earth Sciences, v. 100, p. 1349–1373.

Perrone, G., Eva, E., Cadoppi, P., Solarino, S., and Fioraso, G., 2011b, Seismotectonics of a low-deformation area: the Central Western Alps (Italy): Bollettino di Geofisica Teorica ed Applicata, v. 52, p. 261-281.

Perrone, G., Morelli, M., Piana, F., Fioraso, G., Nicolò, G., Mallen, L., Cadoppi, P., Balestro, G., and Tallone, S., 2013, Current tectonic activity and differential uplift along the Cottian Alps/Po Plain boundary (NW Italy) as derived by PS-InSAR data: Journal of Geodynamics, v. 66, p. 65-78.

Piana, F., 2000, Structural features of western Monferrato (Alps-Apennines junction zone, NW Italy): Tectonics, v. 19, 943–960.

Piana, F., and Polino, R., 1995, Tertiary structural relationships between Alps and Apennines: the critical Torino Hill and Monferrato Area, Northwestern Italy: Terra Nova, v. 7, p. 138-143.

Piana, F., Tallone, S., Cavagna, S. and Conti A., 2006, Thrusting and faulting in metamorphic and sedimentary units of Ligurian Alps. An example of integrated field work and geochemical analyses: International Journal of Earth Sciences, v. 95, 413-430.

Piccardo, G.B., Müntener, O., and Zanetti, A., 2004, Alpine–Apennine ophiolitic peridotites: new concepts on their composition and evolution: Ofioliti, v. 29, p. 63–74.

Platt, J.P., 1993, Exhumation of high-pressure rocks: a review of concepts and processes: Terra Nova, v. 5, p. 119–133.

Pognante, U., 1980, Preliminary data on the Piemonte Ophiolite Nappe in the lower Val Susa - Val Chisone area, western Alps: Ofioliti, v. 5, p. 221-240.

Polino, R., Dal Piaz, G.V., and Gosso, G., 1990, Tectonic erosion at the Adria margin and accretionary processes for the Cretaceous orogeny of the Alps: Mémoires de la Société géologique de France, v. 156, p. 345-367.

Pollard, D.D., Saltzer, S.D., and Rubin, A.M., 1993, Stress inversion methods: are they based on faulty assumptions?: Journal of Structural Geology, v. 15, p. 1045–1054.

Rahn, M., Brandon, M., Batt, G., and Garver, J., 2004, A zero-damage model for fission-track annealing in zircon: American Mineralogist, v. 89, p. 473–484.

Ramsay, J. G., and Huber, M. I., 1987, The Techniques of Modern Structural Geology. Volume 2: Folds and Fractures: London, Academic Press.

Reiners, P.W., and Brandon M.T., 2006, Using thermochronology to understand orogenic erosion: Annual Review of Earth and Planetary Sciences, v. 34, p. 419–466.

Ricou, L.E., and Siddans, W.B., 1986, Collision tectonics in the western Alps. London, Geological Society, Special Publications 19, 229-244.

Rolland, Y., Lardeaux, J.M., Guillot, S., and Nicollet, C., 2000, Extension syn-convergence, poinçonnement vertical et unités métamorphiques contrastées en bordure ouest du Gran Paradis (Alpes Franco-Italiennes): Geodynamica Acta, v. 13, p. 133-148.

Rosenbaum, G., and Lister, G.S., 2005, The Western Alps from the Jurassic to Oligocene: spatio-temporal constraints and evolutionary reconstructions: Earth-Science Reviews, v. 69, p. 281-386.

Rossetti, F., Storti, F., and Läufer, A., 2002, Brittle architecture of the Lanterman Fault and its impact on the final terrane assembly in North Victoria Land, Antarctica: Journal of Geological Society of London, v. 159, p. 159-173.

Roure, F., Polino, R., and Nicolich, R., 1990, Early Neogene deformation beneath the Po Plain: constraints on the post-collisional Alpine evolution: Mémoires de la Société géologique de France, v. 156, p. 309-322.

Sage, F., Beslier, M. O., Thinon, I., Larroque, C., Dessa, J. X., Migeon, S., Angelier, J., Guennoc, P., Schreiber, D., Michaud, F., Stephan, J.-F., Sonnette, L., 2011, Structure and evolution of a passive margin in a compressive environment: Example of the southwestern Alps–Ligurian basin junction during the Cenozoic:. Marine and Petroleum Geology 28, 1263-1282.

Sanchez, G., Rolland, Y., Schreiber, D., Giannerini, G., Corsini M.,and Lardeaux J.M., 2010, The active fault system of SW Alps: Journal of Geodynamics, v. 49, p. 296-302.

Sanderson, D.J., and Marchini, W.R.D., 1984, Transpression: Journal of Structural Geology, v. 6, p. 449–458.

Sandrone, R., and Compagnoni, R., 1977, Il Massiccio Ultrabasico di Lanzo nel quadro del metamorfismo alpino: Rendiconti della Società Italiana di Mineralogia e Petrologia, v. 35, p. 842.

Schmid, S. M., 2004, Tectonic map and overall architecture of the Alpine orogen: Eclogae Geologicae Helvetiae, v. 97, p. 93-117.

Schmid, S.M., and Kissling, E., 2000, The Arc of Western Alps in the light of geophysical data on deep crustal structure: Tectonics, v. 19, p. 62-85.

Schmid, S.M., Zingg, A., and Handy, M., 1987, The kinematics of movements along the Insubric Line and the emplacement of the Ivrea Zone: Tectonophysics, v. 135, p. 47-66.

Schmid, S.M., Aebli, H.R., Heller, F., and Zingg, A., 1989, The role of the Periadriatic Line in the tectonic evolution of the Alps, *in* Coward, M.P., Dietrich, D., and Park, R.G., eds., Alpine Tectonics: London, Geological Society, Special Publications, v. 45, p. 153-171.

Scholz, C.H., 1988, The brittle-plastic transition and the depth of seismic faulting: Geologische Rundschau, v. 77, p. 319-328.

Selverstone, J., 2005, Are the Alps collapsing?: Annual Review of Earth and Planetary Sciences, v. 33, p. 113-132.

Seward, D., and Mancktelow, N.S., 1994, Neogene kinematics of the central and western Alps: Evidence from fission-track dating: Geology, v. 22, p. 803-806.

Sibson, R.H., 1977, Fault rocks and fault mechanisms: Journal of Geological Society of London, v. 133, p. 191-213.

Sommaruga, A., 1999, Dècollement tectonics in the Jura foreland fold and thrust belt: Marine and Petroleum Geology, v. 16, p. 111-134.

Spalla, M.I., De Maria, L., Gosso, G., Miletto, M., and Pognante, U., 1983, Deformazione e metamorfismo della Zona Sesia-Lanzo meridionale al contatto con la Falda Piemontese e con il Massiccio di Lanzo, Alpi Occidentali: Memorie della Società Geologica Italiana, v. 26, p. 499-514.

Storti, F., Rossetti, F., Laüfer, A., and Salvini, F., 2006, Consistent kinematic architecture in the damage zones of intraplate strike-slip fault systems in North Victoria Land, Antarctica and implications for fault zone evolution: Journal of Structural Geology, v. 28, p. 50–63.

Sue, C., and Tricart, P., 1999, Late Alpine brittle extension above the Frontal Pennine Thrust near Briançon, Western Alps: Eclogae Geologicae Helvetiae, v. 92, p. 171-181.

____, 2002, Widespread post-nappe normal faulting in the Internal Western Alps: a new constraint on arc dynamics: Journal of Geological Society of London, v. 159, p. 61-70.

____, 2003, Neogene to current normal faulting in the inner western Alps: A major evolution of the late alpine tectonics: Tectonics, v. 22, p. 1050.

Sue, C., Delacou, B., Champagnac, J.D., Allanic, C., Tricart, P., and Burkhard, M., 2007, Extensional neotectonics around the bend of the Western/Central Alps: an overview: International Journal of Earth Sciences, v. 96, p. 1101-1129.

Sylvester, A.G., 1988, Strike-slip faults: Geological Society of America Bulletin, v. 100, p. 1666–1703.

Tallone, S., Cadoppi, P., Balestro, G., Delle Piane, L., Perello, P., and Riccio, I., 2002, Ductile-to-brittle tectonic evolution at the structural knot between the Lower and Middle Susa Valley (Province of Turin): Congress of the Italian Geological Society, 81th, Turin, Abstracts, p. 310-311.

Tavarnelli, E., 1998, Tectonic evolution of the Northern Salinian Block, California, USA: Palaeogene-to-Recent shortening in a transform fault-bounded continental fragment, *in* Holdsworth, R.,E., Strachan, R., and Dewey, J.,F., eds., Continental transpressional and transtensional tectonics: London, Geological Society, Special Publications, v. 135, p. 107-118.

Tavarnelli, E., and Holdsworth, R.,E., 1999, How long do structures take to form in transpression zones? A cautionary tale from California: Geology, v. 27, p. 1063-1066.

Tavarnelli, E., and Pasqui, V., 2000, Fault growth by segment linkage in seismically active settings: examples from the Southern Apennnines, Italy, and the Coast Ranges, California: Journal of Geodynamics, v. 29, p. 501-516.

Tavarnelli, E., Holdsworth, R. E., Clegg, P., Jones, R. R., and McCaffrey, K. J. W., 2004, The anatomy and evolution of a transpressional imbricate zone, Southern Uplands, Scotland: Journal of Structural Geology, v. 26, p. 1341–1360.

Teyssier, C., Tikoff, B., and Markley, M., 1995, Oblique plate motion and continental tectonics: Geology, v. 23, p. 447–450.

Tikoff, B., and Teyssier, C., 1994, Strain modelling of displacement–field partitioning in transpressional orogens: Journal of Structural Geology, v. 16, p. 1575–1588.

Tikoff, B., and Greene, D., 1997, Stretching lineations in transpressional shear zones: an example from the Sierra Nevada batholith, California: Journal of Structural Geology, v. 19, p. 29–39.

Tikoff, B., Teyssier, C., and Waters, C., 2002, Clutch tectonics and the partial attachment of lithospheric layers, *in* Bertotti, G., Schulmann, K., and Cloetingh, S.A.P.L., eds., Continental Collision and the Tectonosedimentary Evolution of Forelands: EGU Stephan Mueller Special Publication, v. 1, p. 57–73.

Tricart, P., 1984, From passive margin to continental collision: A tectonic scenario for the western Alps: American Journal of Sciences, v. 284, p. 97-120.

____, 2004, From extension to transpression during the final exhumation of the Pelvoux and Argentera massifs, Western Alps: Eclogae Geologicae Helvetiae, v. 97, p. 429-439.

Tricart, P., Schwartz, S., Sue, C., Poupeau, G., and Lardeaux, J.M., 2001, La dénudation tectonique de la zone ultradauphinoise et l'inversion du front briançonnais au sud-est du Pelvoux (Alpes occidentales): Une dynamique Miocène à actuelle: Bulletin de la Société Géologique de France, v. 172, p. 49–58.

Tricart, P., Schwartz, S., Sue, C., and Lardeaux, J.M., 2004, Evidence of synextension tilting and doming during final exhumation from analysis of multistage faults (Queyras Schistes lustrés, Western Alps): Journal of Structural Geology, v. 26, p. 1633-1645.

Tricart, P., Van der Beek, P., Schwartz, S., and Labrin, E. 2007, Diachronous late-stage exhumation across the western Alpine arc: constraints from apatite fission-track termochronology between Pelvoux and Dora-Maira Massifs: Journal of Geological Society of London, v. 164, p. 163-174.

Vanossi, M., Perotti, C., Seno, S., 1994, The Maritime Alps arc in the Ligurian and Tyrrhenian systems: Tectonophysics, v. 230, p. 75-89.

Vauchez, A., Tommasi, A., Barruol, G., 1998, Rheological heterogeneity, mechanical anisotropy and deformation of the continental lithosphere: Tectonophysics, v. 296, p. 61–86.

Vignaroli, G. L., Faccenna, C., Jolivet, L., Piromallo, C., and Rossetti, F., 2008, Subduction polarity reversal at the junction between the Western Alps and the Northern Apennines, Italy: Tectonophysics, v. 450, p. 34–50.

Vigny, C., Chery, J., Duquesnoy, T., et al., 2002, GPS network monitor the western Alps deformation over a five year period: 1993-1998: Journal of Geodesy, v. 76, p. 63-76.

Vollmer, F.W., 1995, C program for automatic contouring of spherical orientation data using a modified Kamb method: Computers & Geosciences, v. 21, p. 31-49.

Wagner, M., Kissling, E., and Husen, S., 2012, Combining controlled-source seismology and local earthquake tomography to derive a 3-D crustal model of the western Alpine region: Geophysical Journal International, v. 191, p. 789-802.

Wilcox, R.E., Harding, T.P., and Seely, D.R., 1973, Basic wrench tectonics: American Association of Petroleum Geologists Bulletin, v. 57, p. 74–96.

Woodcock, N.H., and Fischer, M., 1986, Strike-slip duplexes: Journal of Structural Geology, v. 7, p. 725–735.

Woodcock, N.H., and Schubert, C., 1994, Continental strike-slip tectonics. *in* Hancock, P.L., ed., Continental Tectonics: Pergamon, Oxford, p. 251–263.

Woodcock, N.H., and Rickards, R.B., 2003, Transpressive duplex and flower structure: Dent Fault System, NW England: Journal of Structural Geology, v. 25, p. 1981-1992.

Zoback, M.D., and Healy, J.H., 1992, In situ stress measurements to 3.5 km depth in the Cajon Pass Scientific Research Borehole: implications for the mechanics of crustal faulting: Journal of Geophysical Research, v. 97, p. 5039–5057.

Figure captions:

Figure 1: Map and cross-sections of strike-slip duplexes formed at bends of transcurrent faults. **a)** and **c)** show symmetric flower structures displacing an antiformal push-up or a synformal pull-apart; **b)** shows an asymmetric positive flower structure displacing a monocline. Modified from Woodcock and Rickards (2003).

Figure 2: a) tectonic sketch of the NW Italy (after Bigi *et al.* 1990), the dashed rectangle indicates the area of Figure 2b; **b)** tectonic map of the Cottian-Graian Alps; **c)** ECORS-CROP profile across the Western Alps, trace of the section in Figure 2a; **d)** geological section across the innermost Cottian Alps (after Perrone *et al.* 2011a). AB: Alessandria Basin; GB: Gonfolite Basin; M: Monferrato; SB: Savigliano Basin; TH: Torino Hill; TPB: Tertiary Piemonte Basin; ARL: Aosta-Ranzola Line; AXF: Ax Fault; CFZ: Colle delle Finestre Deformation Zone; CHL: Chamonix Line; CL: Canavese Line; CRL: Cremosina Line; LF: Longitudinal fault system; LTZ: Col del Lis–Trana Deformation Zone; OSL: Ospizio-Sottile Line; OSZ: Orco Shear Zone; PF: Penninic Front; PTF: Padanian Thrust Front; RFDZ: Rio Freddo Deformation Zone; RL: Rodano Line; SAF: Southern Alpine Thrust; SF: Simplon Fault; SSB: Saluzzo-Sommariva del Bosco Thrust; STF: Stura Fault; SVL: Sestri-Voltaggio Line; TF: Transverse Faults; TL: Tonale Line; VVL: Villalvernia-Varzi Line. Fission tracks from Bernet *et al*. (2001).

Figure 3: geological-structural map of the study area; equal-area projections (lower hemisphere) show the mesoscopic scale data relative to (**a**) the faults and (**b**) S_T measured in the study area. In the equal-area plot (**a**) the data collected in the structural stations were not considered. VDZ: Viù Deformation Zone.

Figure 4: geological sections across the mapped area. The traces of the sections are shown in the Fig. 3.

Figure 5: a) interference pattern between D_1 and D_2 folds in albite micaschists; **b**) D_2 isoclinal fold deforming a metre-scale block of leucogneiss; **c**) D_2 fold showing an eye-shaped profile in albite-chlorite-epidote-schists (near Rocca Sapai); **d**) decametre-scale D_3 fold in albite-chlorite-epidote-schists (Rocca Sapai); **e**) interference pattern between D_3 and D_4 folds in the serpentinite schists (Lanzo Ultramafic Complex; Porte di Viù); **f**) type 3 interference pattern between D_2 and D_3 folds in the quartz-micaschists (Viana River); **g**) D_4 open folds in serpentinite schists (Lanzo Ultramafic Complex); **h**) photomicrograph (cross-polarized light) showing the mylonitic structure of the serpentinite schists along the contact between the Lanzo Ultramafic Complex and the SLU.

Figure 6: Digital Elevation Model with the morpho-structural elements of the Lower Viù valley. (1) elbow of capture, (2) deep fluvial incision, (3) wind gap and pass, (4) discontinuity along ridge, (5) straight valley, (6) straight fluvial incision, (7) alignment of peaks.

Figure 7: faults with related slickenlines in the study area. All data were contoured using the modified Kamb method proposed by Vollmer (1995), with $E=2\sigma$ and inverse area smoothing. Contour interval is 2σ beginning at 2σ.

Figure 8: a) detail of the N-S decametre-scale fault zone that juxtaposes the SLU to the Lanzo Ultramafic Complex (south of the Cialmetta pass); synthetical Riedel shears indicate a strong reverse component of movement; **b)** brittle-ductile N-S reverse fault in serpentinites (Lanzo Ultramafic Complex - west of Fubina village); the dashed white line shows the dragging of the schistosity (S_T) along the fault; **c)** conjugate N-S reverse-dextral and NNW-SSE reverse-sinistral faults in serpentinites (Lanzo Ultramafic Complex - west of Fubina village); **d)** brittle-ductile N-S fault in serpentinites (Lanzo Ultramafic Complex – Uja di Calcante);

Figure 9: a) NNE-SSW to NNW-SSE steeply dipping faults showing a positive flower geometry (Lanzo Ultramafic Complex - west of Fubina village); **b)** N-S sub-vertical fault with synthetical Riedel shears indicating a strong reverse component of movement; **c)** antigorite slickenfibres showing right-lateral sense of movement along an N-S fault (south of Cialmetta pass; Lanzo Ultramafic Complex); **d)** N-S reverse faults moderately dipping to the west that drag and displace antigorite veins in serpentinites (south of Cialmetta pass; Lanzo Ultramafic Complex); **e)** N-S normal faults in micaschists (SLU; near Polpresa village); **f)** N-S normal faults cross-cutting the brittle-ductile low-angle thrust fault of Fig. 10d in micaschists (SLU; near Viù village).

Figure 10: a) and **b)** foliated cataclasites, observed in map view, associated with an NNW-SSE sub-vertical fault in serpentinites (Lanzo Ultramafic Complex, south of the Uja di Calcante); synthetical Riedel shears indicate a left-lateral sense of movement; **c)** brittle-ductile low-angle thrust dipping to the ENE, juxtaposing micaschists to metabasites; in the inset, a detail of the structure with sense of movement indicators is shown (near Viù; SLU); **d)** sub-horizontal top to ESE brittle-ductile thrust fault reactivating the schistosity in a decimetre-scale level of chlorite-schists; The equal-area plot between c) and d) shows the senses of movements measured for the low-angle thrust faults. Symbols as in Figure 13.

Figure 11: a) conjugate NW-SE reverse faults in serpentinites (south of Uja di Calcante; Lanzo Ultramafic Complex); **b)** NW-SE sub-vertical fault reactivating the contact between the serpentinite and rodingites; Riedel shears displacing centimetre-scale veins in rodingites indicate a reverse component of movement; **c)** detail of a multi-metre scale tectonic breccias associated with an NW-SE fault (south of the Uja di Calcante; Lanzo Ultramafic Complex); **d)** NW-SE steep to moderately dipping transpressional faults dragging and reactivating the main schistosity in the micaschists (east of Viù; SLU); **e)** NW-SE steeply dipping transpressional faults in serpentinites (south of the Uja di Calcante; Lanzo Ultramafic

Complex); **f)** NE-SW reverse faults in serpentinites schists (west of Fubina; Lanzo Ultramafic Complex).

Figure 12: geometry at different scales of the structures associated with the Viù Deformation Zone. **a)** panoramic view of the study area with a line-drawing showing the km-scale geometry of the major faults; **b)** detail of **a)** showing a fault dipping to the west with a strong reverse component of movement in serpentinites (the Lanzo Ultramafic Complex); **c)** detail of a) showing an N-S transpressional fault zone affecting serpentinites and chlorite schists (50 meters east of the contact between the Lanzo Ultramafic Complex and the SLU); **d)** detail of c) displaying an N-S striking positive flower structure that displaces the contact between chlorite schists and serpentinites.

Figure 13: Fault pattern with the direction of the incremental strain axes obtained at single structural stations. Black numbers in the circles indicate the structural stations. The orientations of the average incremental maximum and minimum strain axes, determined with Bingham distribution statistics, are also shown. VDZ: Viù Deformation Zone. Blue and red arrows indicate structural stations related to the faulting stage 1 and 2 respectively.

Figure 14: a) plan view showing the hierarchical and geometrical relations between the faults associated with the Viù deformation Zone. **b)** pseudo 3D-conceptual block diagram; **c)** simplified structural sketch showing the clockwise rotation of minor faults within the VDZ. Equal-area projections (lower hemisphere) show average kinematic solutions for the different fault systems. The blue and red extensional quadrants in the average kinematic solutions indicate faults associated to the faulting stage 1 and 2 respectively. The thick black great circle indicates the modelled fault plane. For the numerical processing of data, the FaultkinWin software (Allmendinger *et al.* 1991) was used.

Figure 15: a) map of the structural domains of the study area with related equal-area plots showing the distribution of the S_T. Equal-area projections (lower hemisphere) show **(b)** the

distribution of the D_2, D_3 and D_4 fold axes (triangles) and axial surfaces (squares) and **(c)** of the faults measured in each structural domain. VDZ: Viù Deformation Zone.

Figure 16: simplified conceptual model (**a-g**) showing the different stages associated with the development of the Viù Deformation Zone (see text for explanation). In **a)** it is assumed that the LC overlay the SLU and that the S_T slightly dips to the north, as indicated west of the study area by Nicolas *et al.* (1966) and Balestro *et al.* (2009). The images **b1, b2, d1, e1, f1, g1** show mesoscopic scale examples of both ductile syn-metamorphic (**b1, b2**) and brittle structures (**d1**, **e1, f1, g1**) in the different sectors of the study area. **b3)** and **b4)** block models show the geometrical patterns of D_2-D_3-D_4 related folds in the western and eastern sector of the study area, respectively. **b1)** Type 3 interference pattern between D_2 and D_3 folds in the quartz-micaschists (Viana River); **b2)** Type I interference pattern between D_3 and D_4 folds, observable in map-view, in the serpentinite schists (Lanzo Ultramafic Complex; near the Mulapas stream); **d1)** NNE-SSW to NNW-SSE steeply dipping faults showing a positive flower geometry (Lanzo Ultramafic Complex - west of Fubina village); **e1)** antigorite slickenfibres showing right-lateral sense of movement along an N-S fault (south of Cialmetta pass; Lanzo Ultramafic Complex); **f1)** foliated cataclasites associated with an NNW-SSE sub-vertical fault in serpentinites (Lanzo Ultramafic Complex, south of the Uja di Calcante); S-C structures indicate a left-lateral sense of movement; **g1)** detail of the N-S decametre-scale fault zone that juxtaposes the SLU to the Lanzo Ultramafic Complex (south of the Cialmetta pass); S-C structures indicate a strong reverse component of movement.

Figure 17: Tectonic sketches showing two steps of the post-Oligocene to current tectonics in the inner Western Alps and adjoining domains (after Perrone *et al.* 2011a): **a**) the NW-SE convergence, coupled with the anticlockwise rotation, of the Adria plate with respect to the European plate induces a complex strain partitioning within the inner Alpine chain (Oligocene-Early(?) Miocene); **b**) in the inner Western Alps the anticlockwise rotation is

accommodated by dextral movements along the major faults parallel to the trend of the chain, like the LTZ, whereas the convergence is absorbed by E-W right-lateral faults, like the Orco Shear Zone; **d**) the convergence between the Adria and European plate decreases, and gravitational forces become predominant on the rotational boundary movements in the inner Western Alps, inducing an extensional regime (Early(?) Miocene-Present); **e**) in the study area the E-W faults undergo normal reactivation. See Perrone *et al.* (2011a) for the bibliographic references relative to the structural, seismological and geodetic data (see the text for explanation). Equal-area lower hemisphere projections show the cumulative P and T axes relative to the first (**c**) and second (**f**) faulting stages obtained by mesoscopic scale fault measurements. The modified Kamb method proposed by Vollmer (1995), with $E=2\sigma$ and inverse area smoothing was used for the contour. Contour interval is 2σ beginning at 2σ. ARL: Aosta-Ranzola Line; CHL: Chamonix-Rhone Line; CL: Canavese Line; CRL: Cremosina Line; DM: Dora-Maira Unit; GP: Gran Paradiso Unit; HF: Helvetic Front; LF: Longitudinal Faults; LTZ: Col del Lis-Trana Deformation Zone; OSZ: Orco shear zone; PT: Penninic Thrust Front; PLU: Piemonte-Ligurian Units; SA: South-Alpine Units; SAT: South-Alpine Thrust; SF: Simplon Fault; SZ: Sesia-Lanzo Zone; TF: Transverse Faults; VDZ: Viù Deformation Zone. Reference indexes on the map are (1) Champagnac *et al.* (2004), (2) Perello *et al.* (2004), (3) Perello *et al.* (1999), (4) Seward and Mancktelow (1994), (5) this study, (6) Balestro *et al.* (2009), (7) Sue and Tricart (2003), (8) Labaume *et al.* (1989), (9) Baietto *et al.* (2009), (10) Mancktelow (1992), (11) Bistacchi *et al.* (2000), (12) Sue and Tricart (1999), (13) Champagnac *et al.* (2006), (14) Tricart *et al.* (2004), (15) Ceriani and Schmid (2004), (16) Eva *et al.* (1997), (17) Delacou *et al.* (2004), (18) Calais *et al.* (2002), (19) Vigny *et al.* (2002), (20) Kastrup *et al.* (2004), (21) Sue *et al.* (1999), (22) Malusa` *et al.* (2009), (23) Fusetti *et al.* (2012), (24) Federico *et al.* (2013), (25) Maino *et al.* (2013), (26) Piana (2000), (27) Festa *et al.* (2015), (28) Dumont *et al.* (2012), (29) Festa *et al.* (2009), (30)

Mosca *et al.* (2009), (31) Tallone *et al.* 2002; (32) Piana *et al.* (2006), (33) Bauve *et al.* (2014).

Figure 18: a) tectonic sketch map of the Western Alps. The thick dashed red line indicates the outline of the Ivrea body whereas the dashed blue line indicates the Viù-Locana Zone. b) Cross-section showing the geometrical relation between LTZ and Ivrea body. LTZ: Col del Lis-Trana Deformation Zone; CABF: Cottian Alps Border Fault; CL: Canavese Line. Outline of the Ivrea body from Wagner *et al.* (2012). The geometry of the Ivrea body in cross-section are based on the tomographic data of and Paul *et al.* (2001); Lardeaux *et al.* 2006; Bethoux *et al.* (2007).

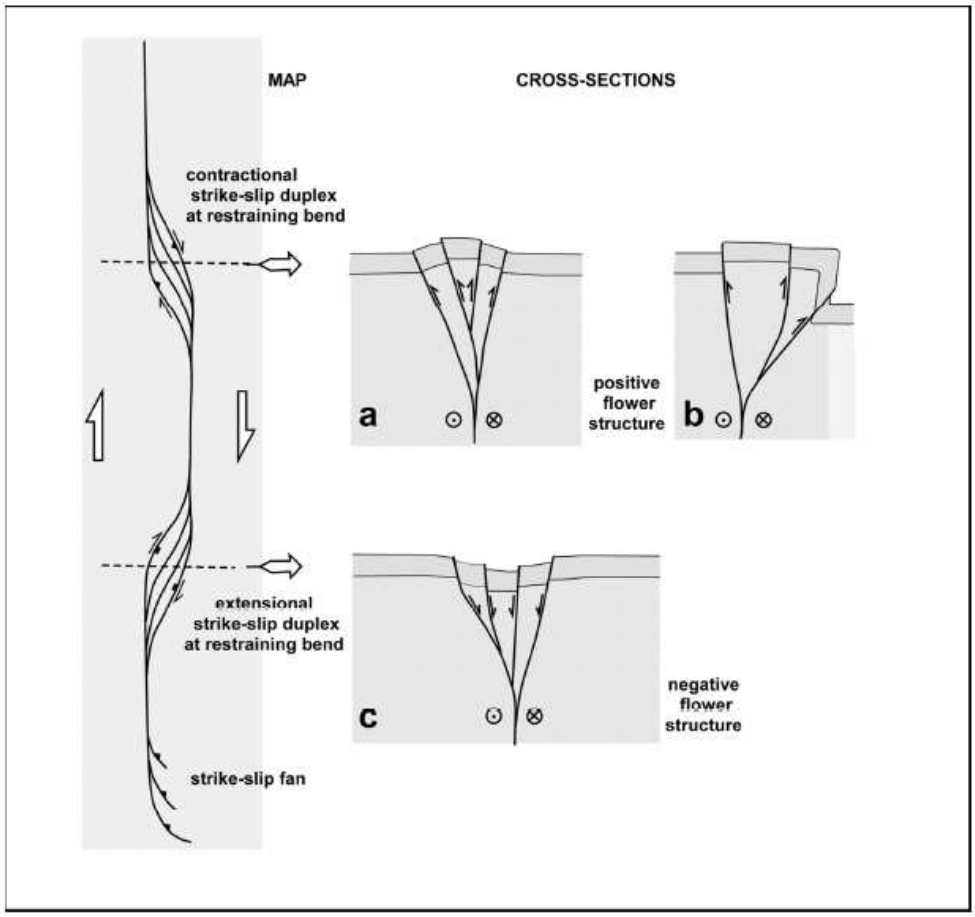

Figure 1: Map and cross-sections of strike-slip duplexes formed at bends of transcurrent faults. a) and c) show symmetric flower structures displacing an antiformal push-up or a synformal pull-apart; b) shows an asymmetric positive flower structure displacing a monocline. Modified from Woodcock and Rickards (2003).
129x122mm (300 x 300 DPI)

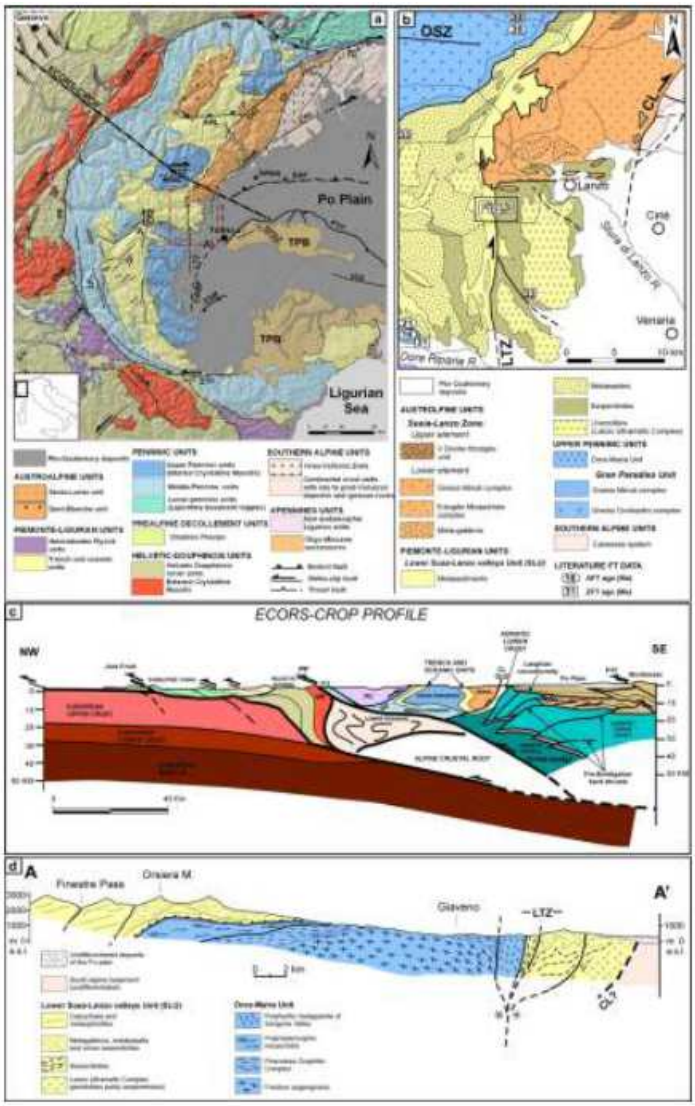

Figure 2: tectonic sketch of the NW Italy (after Bigi et al. 1990), the dashed rectangle indicates the area of Figure 2b; b) tectonic map of the Cottian-Graian Alps; c) ECORS-CROP profile across the Western Alps, trace of the section in Figure 2a; d) geological section across the innermost Cottian Alps (after Perrone et al. 2011a). AB: Alessandria Basin; GB: Gonfolite Basin; M: Monferrato; SB: Saviqliano Basin; TH: Torino Hill; TPB: Tertiary Piemonte Basin; ARL: Aosta-Ranzola Line; AXF: Ax Fault; CFZ: Colle delle Finestre Deformation Zone; CHL: Chamonix Line; CL: Canavese Line; CRL: Cremosina Line; LF: Longitudinal fault system; LTZ: Col del Lis–Trana Deformation Zone; OSL: Ospizio-Sottile Line; OSZ: Orco Shear Zone; PF: Penninic Front; PTF: Padanian Thrust Front; RFDZ: Rio Freddo Deformation Zone; RL: Rodano Line; SAF: Southern Alpine Thrust; SF: Simplon Fault; SSB: Saluzzo-Sommariva del Bosco Thrust; STF: Stura Fault; SVL: Sestri-Voltaggio Line; TF: Transverse Faults; TL: Tonale Line; VVL: Villalvernia-Varzi Line. Fission tracks from Bernet et al. (2001).

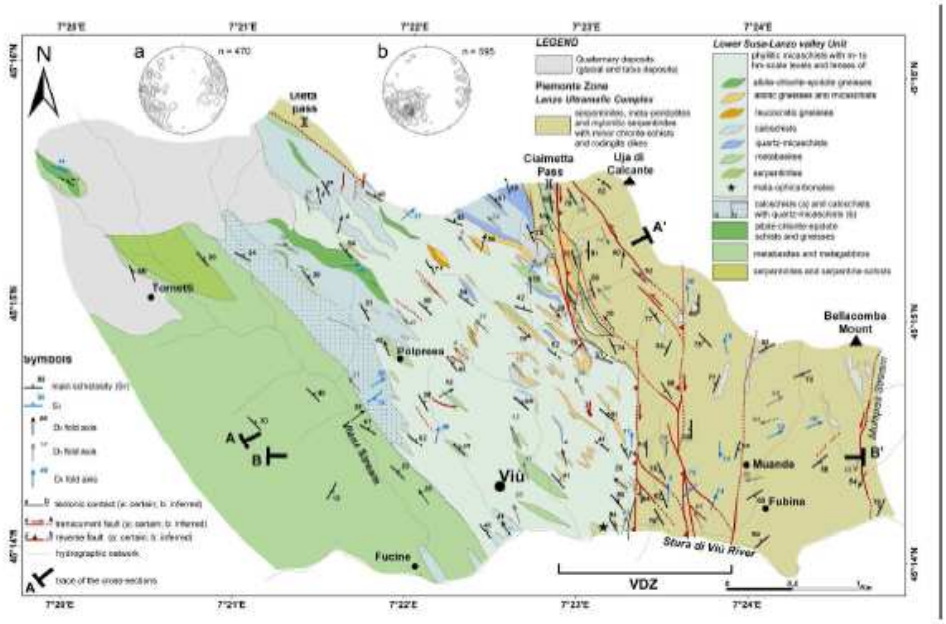

Figure 3: geological-structural map of the study area; equal-area projections (lower hemisphere) show the mesoscopic scale data relative to (a) the faults and (b) ST measured in the study area. In the equal-area plot (a) the data collected in the structural stations were not considered. VDZ: Viù Deformation Zone.

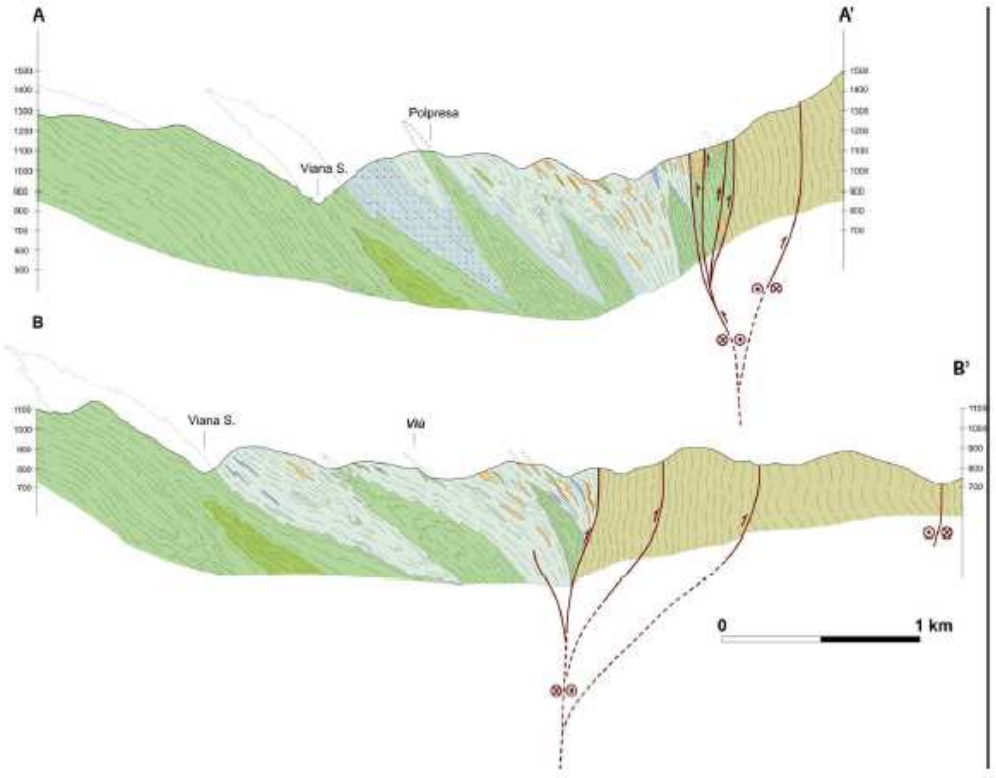

Figure 4: geological sections across the mapped area. The traces of the sections are shown in the Fig. 3.

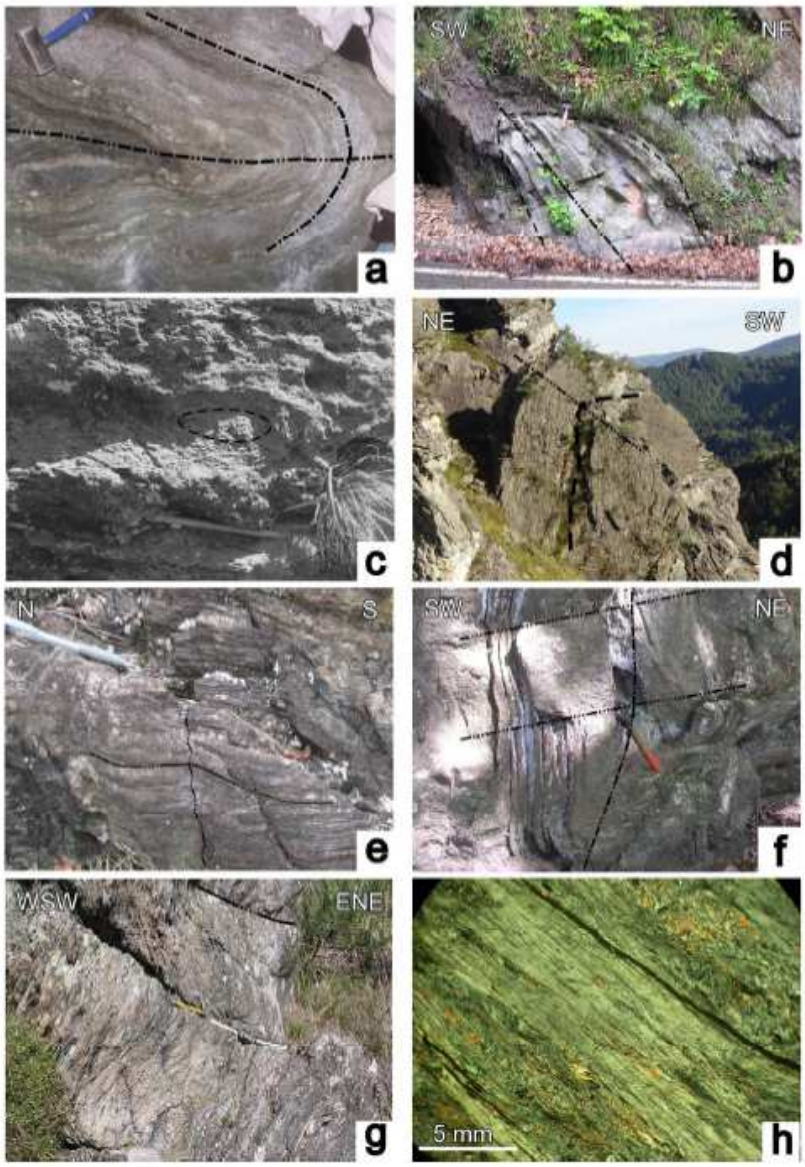

Figure 5: a) interference pattern between D1 and D2 folds in albite micaschists; b) D2 isoclinal fold deforming a metre-scale block of leucogneiss; c) D2 fold showing an eye-shaped profile in albite-chlorite-epidote-schists (near Rocca Sapai); d) decametre-scale D3 fold in albite-chlorite-epidote-schists (Rocca Sapai); e) interference pattern between D3 and D4 folds in the serpentinite schists (Lanzo Ultramafic Complex; Porte di Viù); f) type 3 interference pattern between D2 and D3 folds in the quartz-micaschists (Viana River); g) D4 open folds in serpentinite schists (Lanzo Ultramafic Complex); h) photomicrograph (cross-polarized light) showing the mylonitic structure of the serpentinite schists along the contact between the Lanzo Ultramafic Complex and the SLU.

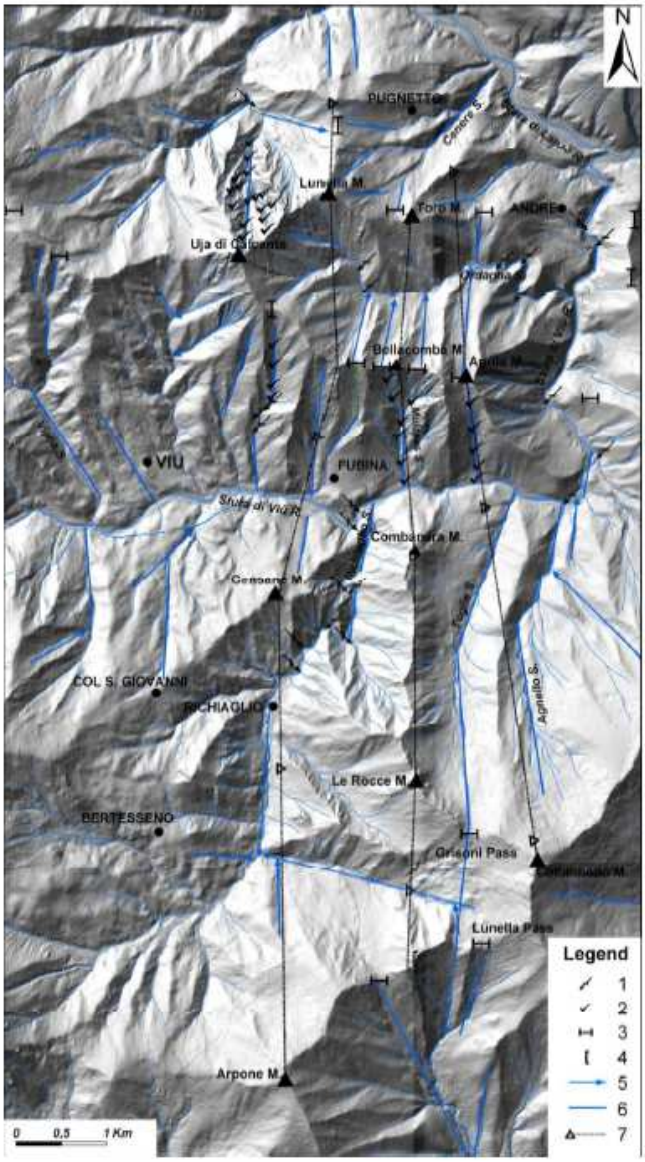

Figure 6: Digital Elevation Model with the morpho-structural elements of the Lower Viù valley. (1) elbow of capture, (2) deep fluvial incision, (3) wind gap and pass, (4) discontinuity along ridge, (5) straight valley, (6) straight fluvial incision, (7) alignment of peaks.

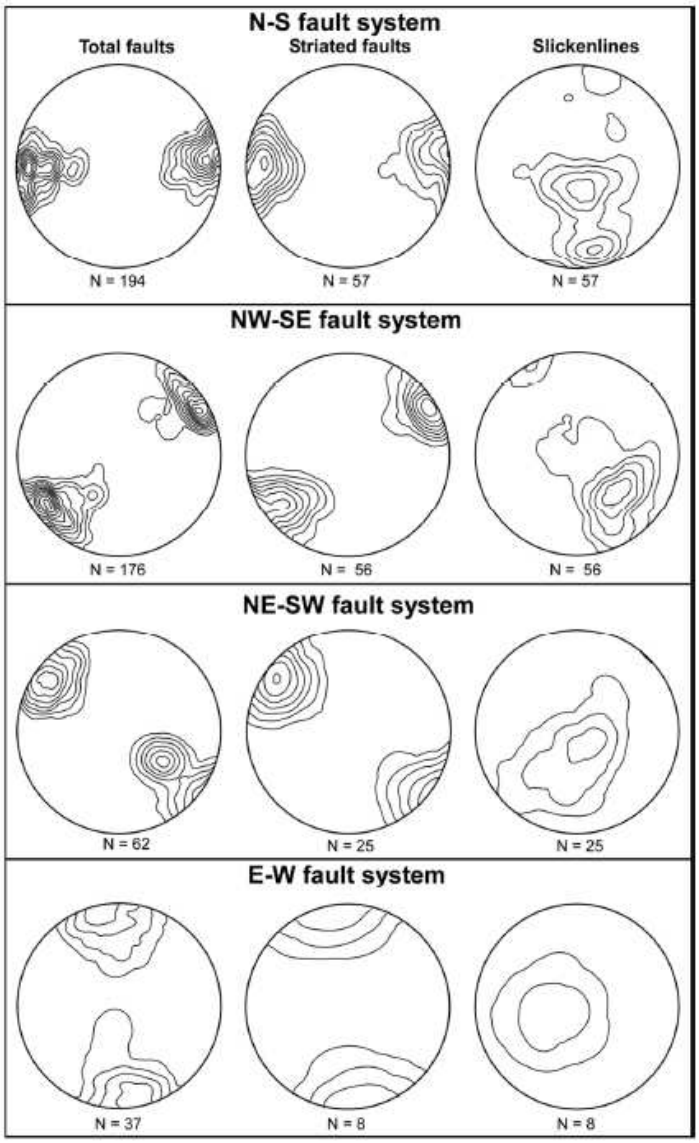

Figure 7: faults with related slickenlines in the study area. All data were contoured using the modified Kamb method proposed by Vollmer (1995), with E=2σ and inverse area smoothing. Contour interval is 2σ beginning at 2σ

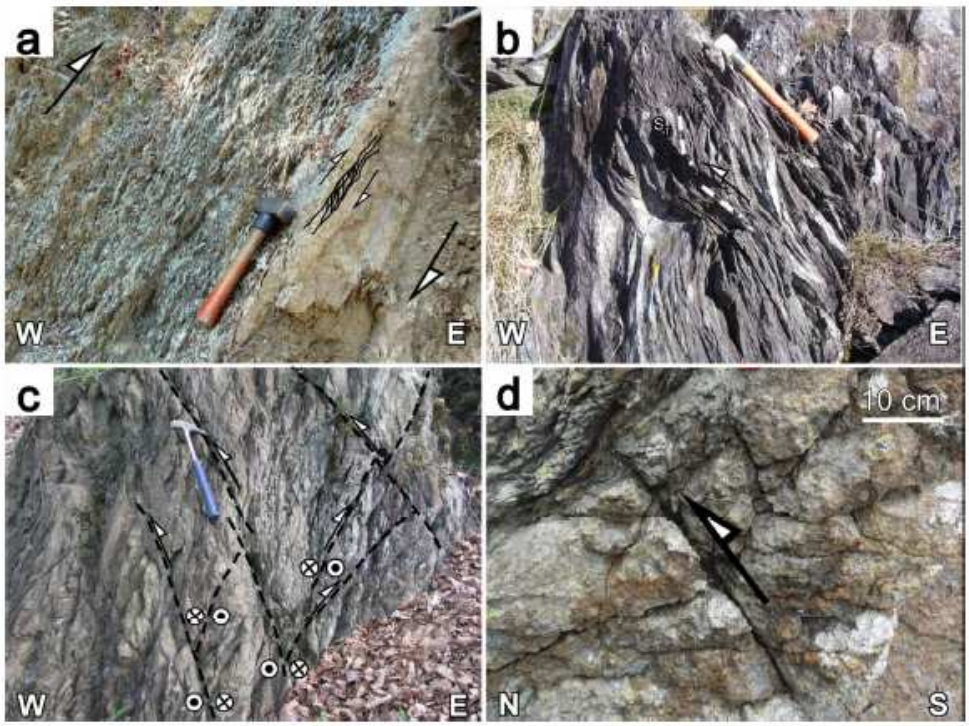

Figure 8: a) detail of the N-S decametre-scale fault zone that juxtaposes the SLU to the Lanzo Ultramafic Complex (south of the Cialmetta pass); synthetical Riedel shears indicate a strong reverse component of movement; b) brittle-ductile N-S reverse fault in serpentinites (Lanzo Ultramafic Complex - west of Fubina village); the dashed white line shows the dragging of the schistosity (ST) along the fault; c) conjugate N-S reverse-dextral and NNW-SSE reverse-sinistral faults in serpentinites (Lanzo Ultramafic Complex - west of Fubina village); d) brittle-ductile N-S fault in serpentinites (Lanzo Ultramafic Complex – Uja di Calcante);

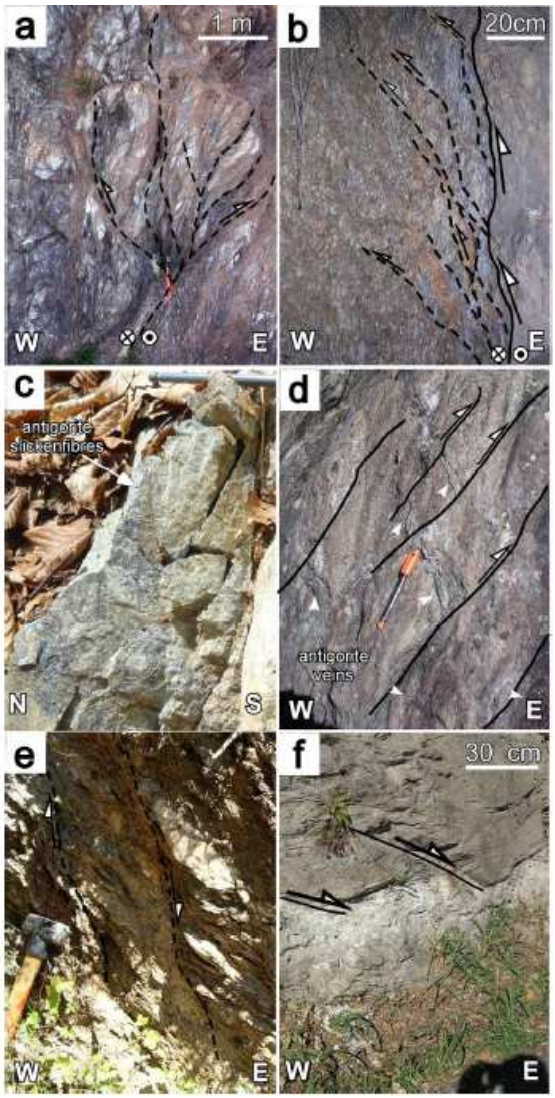

Figure 9: a) NNE-SSW to NNW-SSE steeply dipping faults showing a positive flower geometry (Lanzo Ultramafic Complex - west of Fubina village); b) N-S sub-vertical fault with synthetical Riedel shears indicating a strong reverse component of movement; c) antigorite slickenfibres showing right-lateral sense of movement along an N-S fault (south of Cialmetta pass; Lanzo Ultramafic Complex); d) N-S reverse faults moderately dipping to the west that drag and displace antigorite veins in serpentinites (south of Cialmetta pass; Lanzo Ultramafic Complex); e) N-S normal faults in micaschists (SLU; near Polpresa village); f) N-S normal faults cross-cutting the brittle-ductile low-angle thrust fault of Fig. 10d in micaschists (SLU; near Viù village).

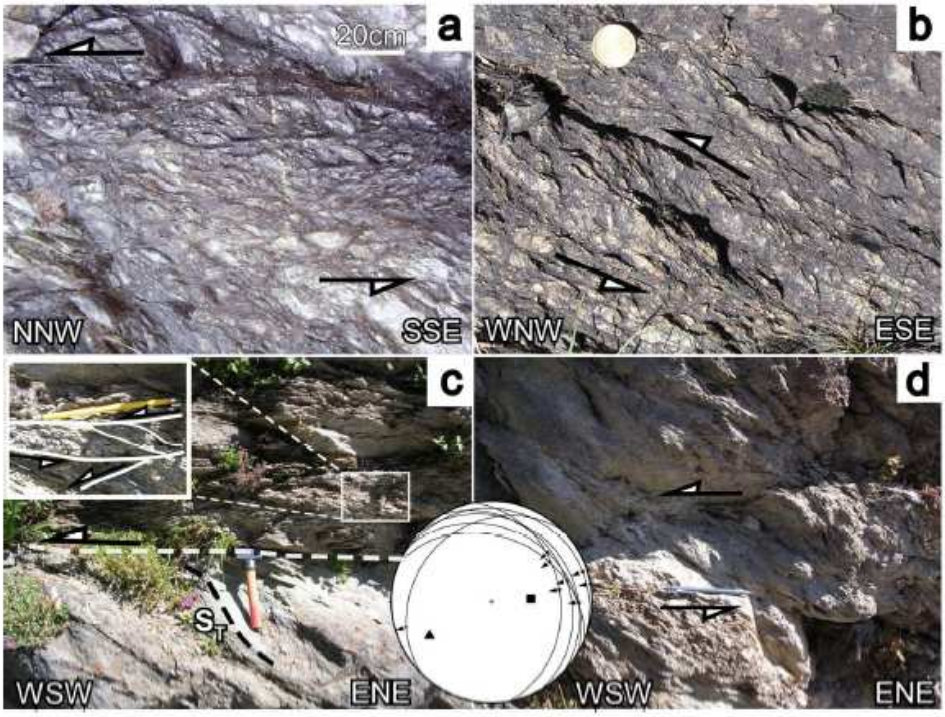

Figure 10: a) and b) foliated cataclasites, observed in map view, associated with an NNW-SSE sub-vertical fault in serpentinites (Lanzo Ultramafic Complex, south of the Uja di Calcante); synthetical Riedel shears indicate a left-lateral sense of movement; c) brittle-ductile low-angle thrust dipping to the ENE, juxtaposing micaschists to metabasites; in the inset, a detail of the structure with sense of movement indicators is shown (near Viù; SLU); d) sub-horizontal top to ESE brittle-ductile thrust fault reactivating the schistosity in a decimetre-scale level of chlorite-schists; The equal-area plot between c) and d) shows the senses of movements measured for the low-angle thrust faults. Symbols as in Figure 13.

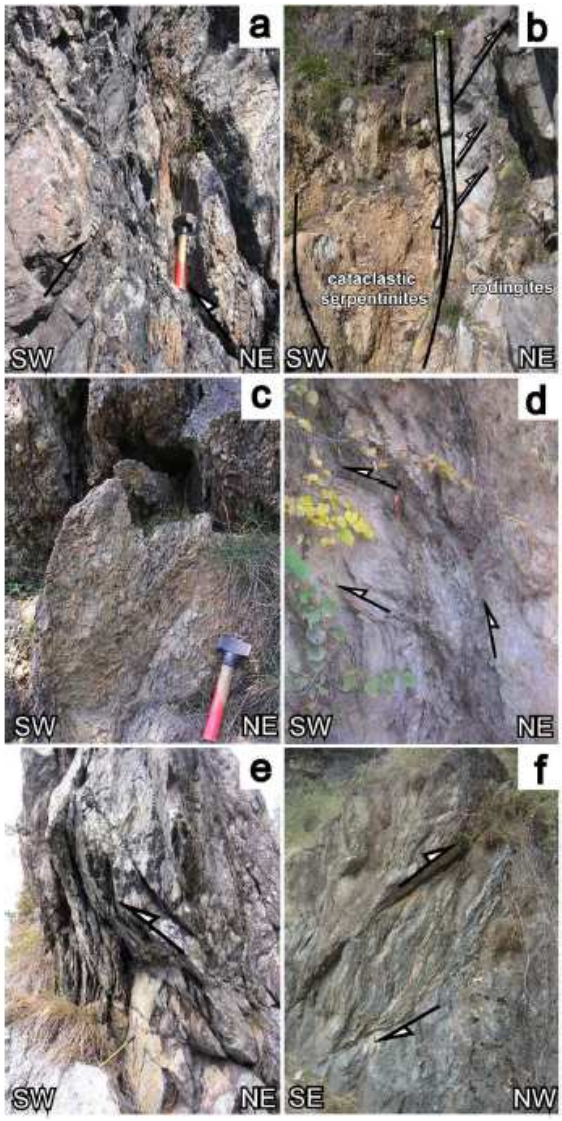

Figure 11: a) conjugate NW-SE reverse faults in serpentinites (south of Uja di Calcante; Lanzo Ultramafic Complex); b) NW-SE sub-vertical fault reactivating the contact between the serpentinite and rodingites; Riedel shears displacing centimetre-scale veins in rodingites indicate a reverse component of movement; c) detail of a multi-metre scale tectonic breccias associated with an NW-SE fault (south of the Uja di Calcante; Lanzo Ultramafic Complex); d) NW-SE steep to moderately dipping transpressional faults dragging and reactivating the main schistosity in the micaschists (east of Viù; SLU); e) NW-SE steeply dipping transpressional faults in serpentinites (south of the Uja di Calcante; Lanzo Ultramafic Complex); f) NE-SW reverse faults in serpentinites schists (west of Fubina; Lanzo Ultramafic Complex).

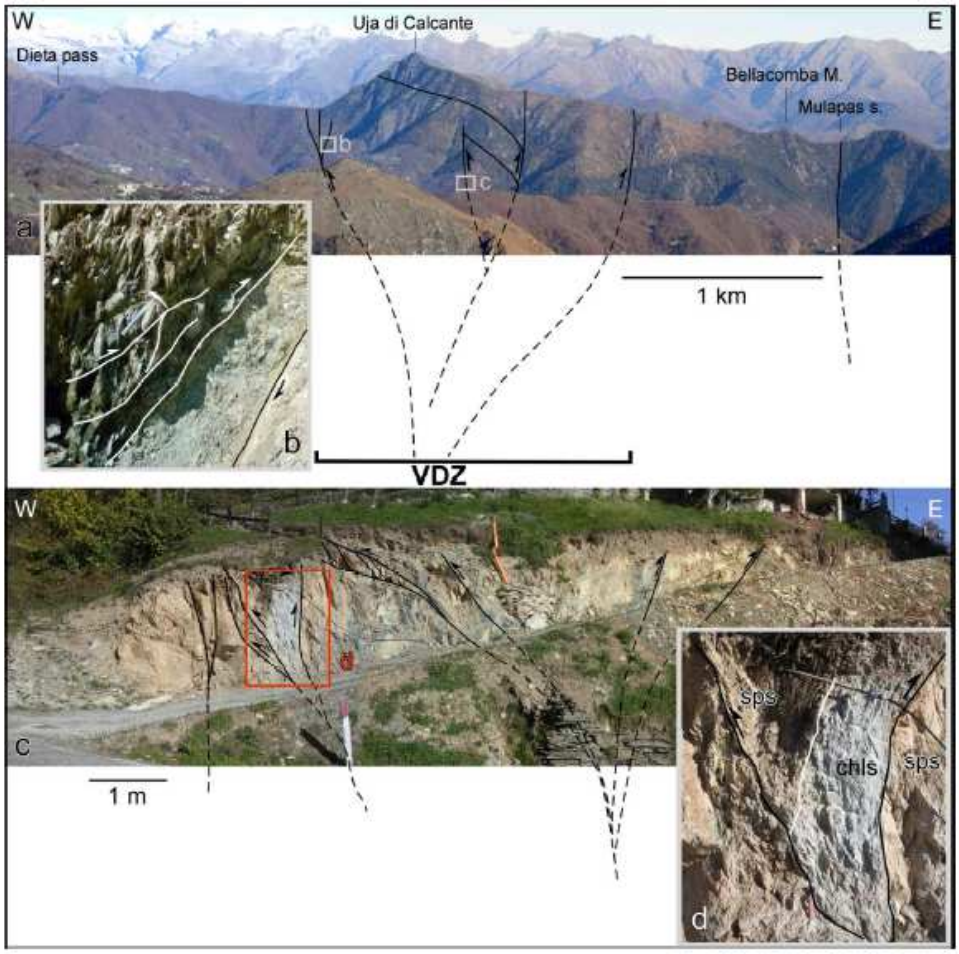

Figure 12: geometry at different scales of the structures associated with the Viù Deformation Zone. a) panoramic view of the study area with a line-drawing showing the km-scale geometry of the major faults; b) detail of a) showing a fault dipping to the west with a strong reverse component of movement in serpentinites (the Lanzo Ultramafic Complex); c) detail of a) showing an N-S transpressional fault zone affecting serpentinites and chlorite schists (50 meters east of the contact between the Lanzo Ultramafic Complex and the SLU); d) detail of c) displaying an N-S striking positive flower structure that displaces the contact between chlorite schists and serpentinites.

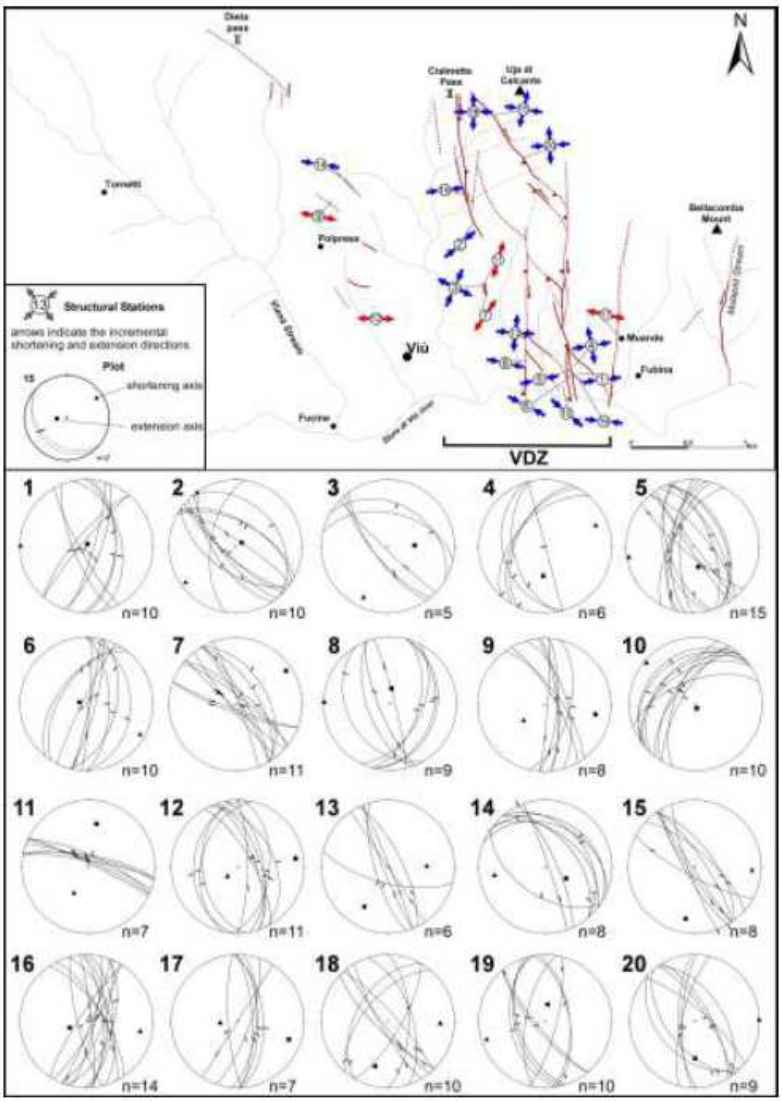

Figure 13: Fault pattern with the direction of the incremental strain axes obtained at single structural stations. Black numbers in the circles indicate the structural stations. The orientations of the average incremental maximum and minimum strain axes, determined with Bingham distribution statistics, are also shown. VDZ: Viù Deformation Zone. Blue and red arrows indicate structural stations related to the faulting stage 1 and 2 respectively.

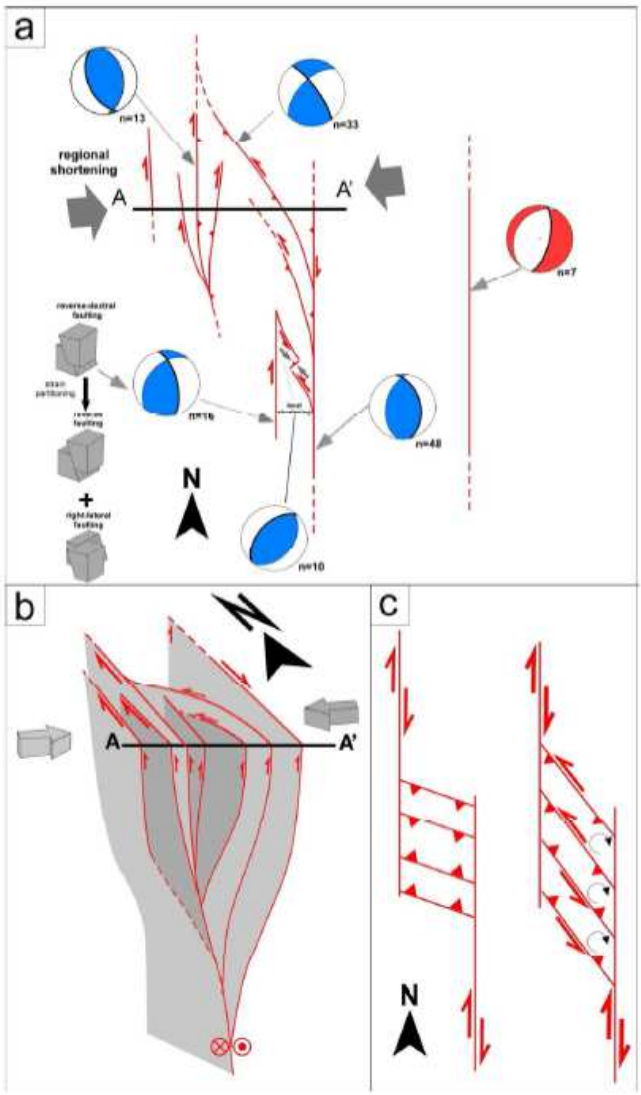

Figure 14: a) plan view showing the hierarchical and geometrical relations between the faults associated with the Viù deformation Zone. b) pseudo 3D-conceptual block diagram; c) simplified structural sketch showing the clockwise rotation of minor faults within the VDZ. Equal-area projections (lower hemisphere) show average kinematic solutions for the different fault systems. The blue and red extensional quadrants in the average kinematic solutions indicate faults associated to the faulting stage 1 and 2 respectively. The thick black great circle indicates the modelled fault plane. For the numerical processing of data, the FaultkinWin software (Allmendinger et al. 1991) was used.

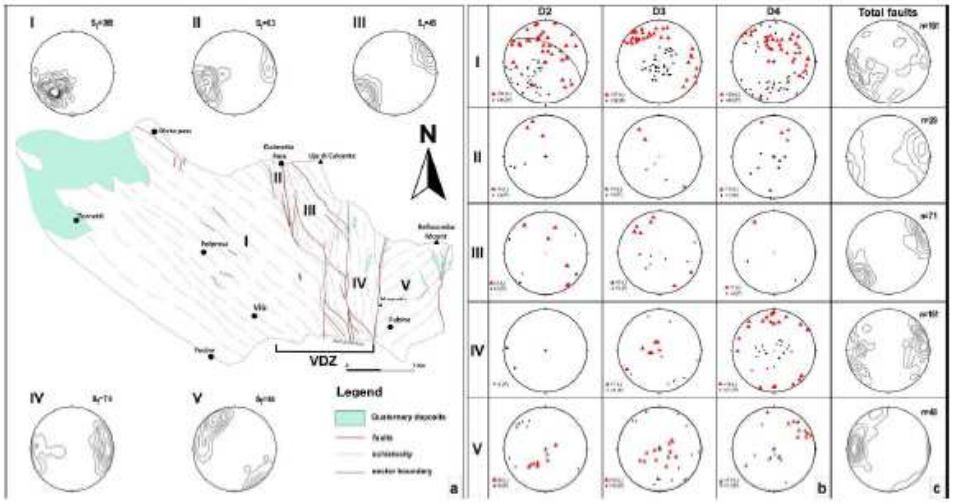

Figure 15: a) map of the structural domains of the study area with related equal-area plots showing the distribution of the ST. Equal-area projections (lower hemisphere) show (b) the distribution of the D2, D3 and D4 fold axes (triangles) and axial surfaces (squares) and (c) of the faults measured in each structural domain. VDZ: Viù Deformation Zone.

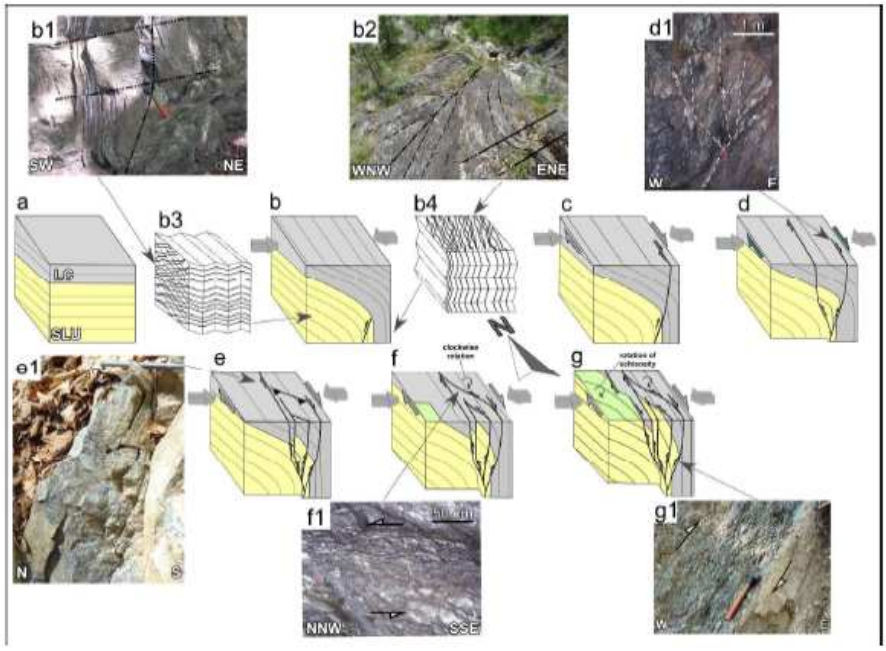

Figure 16: simplified conceptual model (a-g) showing the different stages associated with the development of the Viù Deformation Zone (see text for explanation). In a) it is assumed that the LC overlay the SLU and that the ST slightly dips to the north, as indicated west of the study area by Nicolas et al. (1966) and Balestro et al. (2009). The images b1, b2, d1, e1, f1, g1 show mesoscopic scale examples of both ductile syn-metamorphic (b1, b2) and brittle structures (d1, e1, f1, g1) in the different sectors of the study area. b3) and b4) block models show the geometrical patterns of D2-D3-D4 related folds in the western and eastern sector of the study area, respectively. b1) Type 3 interference pattern between D2 and D3 folds in the quartz-micaschists (Viana River); b2) Type I interference pattern between D3 and D4 folds, observable in map-view, in the serpentinite schists (Lanzo Ultramafic Complex; near the Mulapas stream); d1) NNE-SSW to NNW-SSE steeply dipping faults showing a positive flower geometry (Lanzo Ultramafic Complex - west of Fubina village); e1) antigorite slickenfibres showing right-lateral sense of movement along an N-S fault (south of Cialmetta pass; Lanzo Ultramafic Complex); f1) foliated cataclasites associated with an NNW-SSE sub-vertical fault in serpentinites (Lanzo Ultramafic Complex, south of the Uja di Calcante); S-C structures indicate a left-lateral sense of movement; g1) detail of the N-S decametre-scale fault zone that juxtaposes the SLU to the Lanzo Ultramafic Complex (south of the Cialmetta pass); S-C structures indicate a strong reverse component of movement.

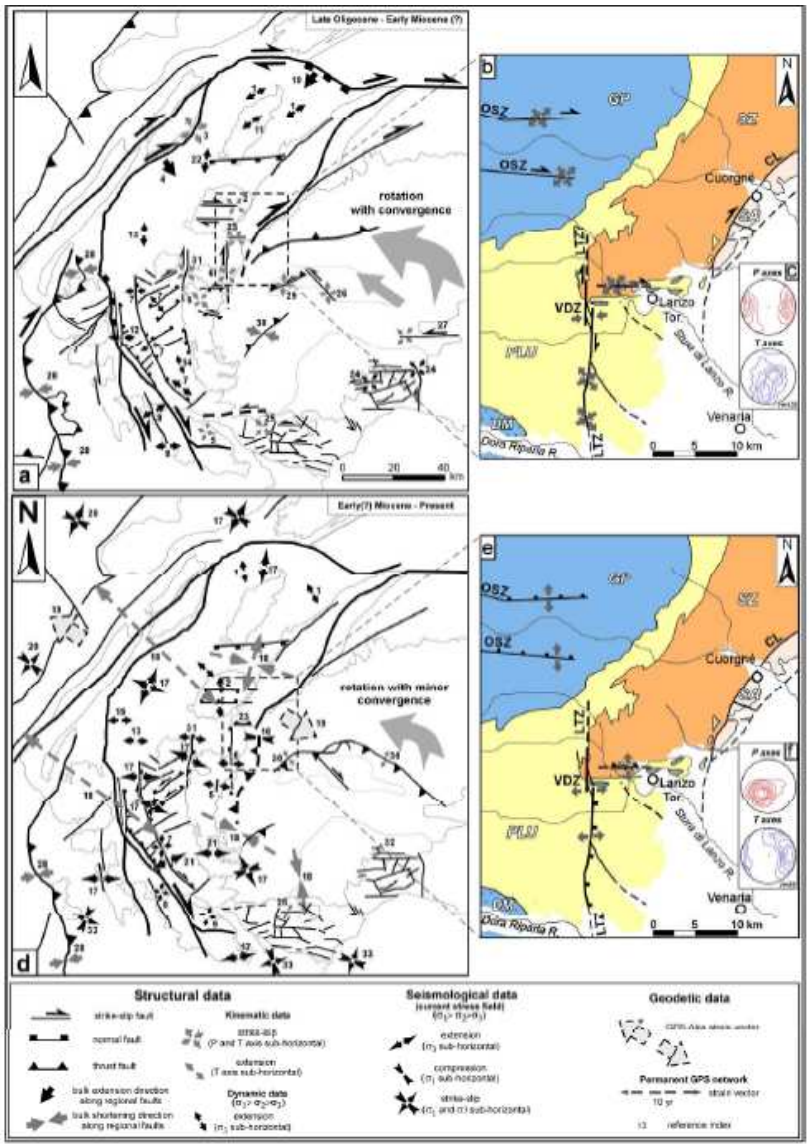

Figure 17: Tectonic sketches showing two steps of the post-Oligocene to current tectonics in the inner Western Alps and adjoining domains (after Perrone et al. 2011a): a) the NW-SE convergence, coupled with the anticlockwise rotation, of the Adria plate with respect to the European plate induces a complex strain partitioning within the inner Alpine chain (Oligocene-Early(?) Miocene); b) in the inner Western Alps the anticlockwise rotation is accommodated by dextral movements along the major faults parallel to the trend of the chain, like the LTZ, whereas the convergence is absorbed by E-W right-lateral faults, like the Orco Shear Zone; d) the convergence between the Adria and European plate decreases, and gravitational forces become predominant on the rotational boundary movements in the inner Western Alps, inducing an extensional regime (Early(?) Miocene-Present); e) in the study area the E-W faults undergo normal reactivation. See Perrone et al. (2011a) for the bibliographic references relative to the structural, seismological and geodetic data (see the text for explanation). Equal-area lower hemisphere projections show the cumulative P and T axes relative to the first (c) and second (f) faulting stages obtained by mesoscopic scale fault measurements. The modified Kamb method proposed by Vollmer (1995), with E=2σ

and inverse area smoothing was used for the contour. Contour interval is 2σ beginning at 2σ. ARL: Aosta-Ranzola Line; CHL: Chamonix-Rhone Line; CL: Canavese Line; CRL: Cremosina Line; DM: Dora-Maira Unit; GP: Gran Paradiso Unit; HF: Helvetic Front; LF: Longitudinal Faults; LTZ: Col del Lis-Trana Deformation Zone; OSZ: Orco shear zone; PT: Penninic Thrust Front; PLU: Piemonte-Ligurian Units; SA: South-Alpine Units; SAT: South-Alpine Thrust; SF: Simplon Fault; SZ: Sesia-Lanzo Zone; TF: Transverse Faults; VDZ: Viù Deformation Zone. Reference indexes on the map are (1) Champagnac et al. (2004), (2) Perello et al. (2004), (3) Perello et al. (1999), (4) Seward and Mancktelow (1994), (5) this study, (6) Balestro et al. (2009), (7) Sue and Tricart (2003), (8) Labaume et al. (1989), (9) Baietto et al. (2009), (10) Mancktelow (1992), (11) Bistacchi et al. (2000), (12) Sue and Tricart (1999), (13) Champagnac et al. (2006), (14) Tricart et al. (2004), (15) Ceriani and Schmid (2004), (16) Eva et al. (1997), (17) Delacou et al. (2004), (18) Calais et al. (2002), (19) Vigny et al. (2002), (20) Kastrup et al. (2004), (21) Sue et al. (1999), (22) Malusa` et al. (2009), (23) Fusetti et al. (2012), (24) Federico et al. (2013), (25) Maino et al. (2013), (26) Piana (2000), (27) Festa et al. (2015), (28) Dumont et al. (2012), (29) Festa et al. (2009), (30) Mosca et al. (2009), (31) Tallone et al. 2002; (32) Piana et al. (2006), (33) Bauve et al. (2014).